Mechanics of fiber composites

2

Levent Aydin[*], *Hatice Seçil Artem*[†], *Erkan Oterkus*[‡], *Omer Gundogdu*[§], *Hamit Akbulut*[§]
[*]Izmir Katip Çelebi University, Izmir, Turkey, [†]Izmir Institute of Technology, Izmir, Turkey, [‡]University of Strathclyde, Glasgow, United Kingdom, [§]Ataturk University, Erzurum, Turkey

2.1 Introduction

The objective of this chapter is to emphasize the context in which the mechanics of fiber composites is examined. Constitutive equations describing the stress-strain relations, micromechanics and macromechanics approaches for mechanical analysis are reviewed. Since interfacial mechanics of composites is of primary importance in discussing the material behavior, this concept is also presented with its constitutive and governing equations. Finally, at the end of the chapter, strength failure theories for orthotropic materials and dynamic behavior of composites are discussed.

The mechanics of materials contended with stresses, strains, and deformations in engineering structures subjected to mechanical, thermal, and hygral loadings. A common assumption in the mechanics of conventional materials, such as steel and aluminum, is that they are homogeneous and isotropic [1]. However, fiber-reinforced composites are inhomogeneous and nonisotropic. As a result, the analysis of the mechanics of fiber-reinforced composites is much more complex than that of conventional materials. The mechanics of fiber-reinforced composite materials is mainly studied at two levels: (1) micromechanics level, in which the interaction of the constituent materials is examined on a microscopic scale. In micromechanical analysis, stiffness, strength, thermal, and moisture expansion coefficients of a lamina are found using the individual properties of constituents (fiber and matrix), (2) macromechanics level, in which the response of a fiber-reinforced composite material to mechanical and thermal loads is studied on a macroscopic scale. The material is assumed to be homogeneous. Stresses, strains, and deflections are determined using the equations of orthotropic elasticity.

2.2 Mechanics of continuous fiber-reinforced composites

Composites are materials in which a homogeneous matrix component is reinforced by a stronger and stiffer constituent that is usually continuous or short fibers. Continuous fiber-matrix composite materials include unidirectional or woven fiber laminae; laminae are stacked on top of each other at various angles to form a multidirectional laminate. The mechanical analysis of fiber-reinforced composites is performed in two levels: micromechanical and macromechanical analyzes.

In the following parts, micromechanical and macromechanical analyzes of continuous-fiber-reinforced composites have been introduced based on classical lamination theory.

Fiber Technology for Fiber-Reinforced Composites. http://dx.doi.org/10.1016/B978-0-08-101871-2.00002-3

2.2.1 Macromechanical analysis

2.2.1.1 Constitutive equations

The classical lamination theory based on Kirchoff's hypothesis is used to analyze the infinitesimal deformation of thin-laminated structures. In this theory, it is assumed that the laminate is thin and wide, layers are perfectly bonded, the material of each layer is linearly elastic and has a uniform thickness, and there exists a linear strain distribution through the thickness (small deformation). Thin-laminated structure subjected to mechanical in-plane loading is shown in Fig. 2.1. Cartesian coordinate system x, y, and z define global coordinates of the layered material. A layerwise principal material coordinate system is denoted by 1, 2, and 3, and fiber direction is oriented at angle θ to the x-axis [2,3].

Based on the theory, the resulting displacement field is then expressed as

$$\begin{aligned} u(x,y,z) &= u_0(x,y) - z\frac{\partial w_0}{\partial x} \\ v(x,y,z) &= v_0(x,y) - z\frac{\partial w_0}{\partial y}(x,y) \\ w(x,y,z) &= w_0(x,y) \end{aligned} \tag{2.1}$$

where u_0, v_0, w_0 are the displacement components along x, y, and z coordinate directions of a point on the midplane ($z=0$), respectively (Fig. 2.2).

Eq. (2.1) implies that straight lines normal to geometric midplane before deformation remain straight after deformation. In this regard, transverse normal strain (ε_{zz}) and shear components (γ_{xz} and γ_{yz}) become zero, and the strain field is then expressed as

$$\begin{aligned} \varepsilon_{xx} &= \frac{\partial u_0}{\partial x} - z\left(\frac{\partial^2 w_0}{\partial x^2}\right) \\ \varepsilon_{yy} &= \frac{\partial v_0}{\partial y} - z\left(\frac{\partial^2 w_0}{\partial y^2}\right) \\ \gamma_{xy} &= \left(\frac{\partial u_0}{\partial y} + \frac{\partial v_0}{\partial x}\right) - 2z\frac{\partial^2 w_0}{\partial x \partial y} \end{aligned} \tag{2.2}$$

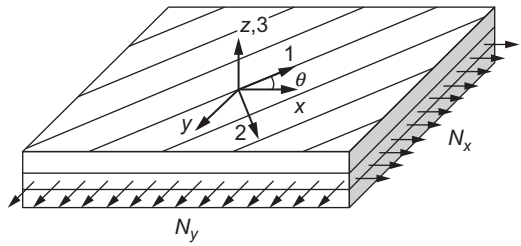

Fig. 2.1 A thin fiber-reinforced laminated composite subjected to in-plane loading [2].

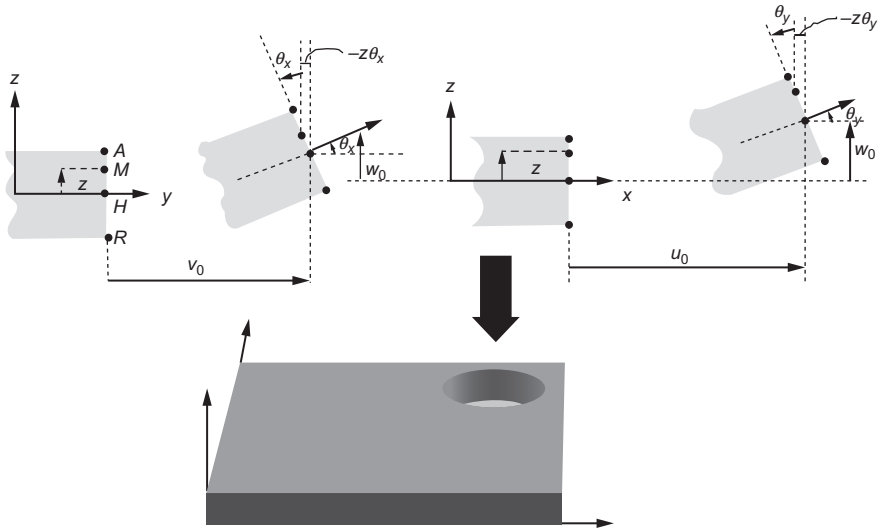

Fig. 2.2 Deformation in the case of classical theory of laminates [4].

Therefore, the nonzero three strains in generalized form including mechanical (M), thermal (T), and hygral (H) effects can be represented as in the following form [2]:

$$\begin{bmatrix} \varepsilon_{xx} \\ \varepsilon_{yy} \\ \gamma_{xy} \end{bmatrix} = \begin{bmatrix} \varepsilon_{xx}^{M} \\ \varepsilon_{yy}^{M} \\ \gamma_{xy}^{M} \end{bmatrix} + \begin{bmatrix} \varepsilon_{xx}^{T} \\ \varepsilon_{yy}^{T} \\ \gamma_{xy}^{T} \end{bmatrix} + \begin{bmatrix} \varepsilon_{xx}^{H} \\ \varepsilon_{yy}^{H} \\ \gamma_{xy}^{H} \end{bmatrix} \tag{2.3}$$

where

$$\begin{bmatrix} \varepsilon_{xx} \\ \varepsilon_{yy} \\ \gamma_{xy} \end{bmatrix} = \begin{bmatrix} \varepsilon_{xx}^{0} \\ \varepsilon_{yy}^{0} \\ \gamma_{xy}^{0} \end{bmatrix} + z \begin{bmatrix} \kappa_{xx} \\ \kappa_{yy} \\ \kappa_{xy} \end{bmatrix}$$

Here, the midplane strain matrix and the curvature matrix of the laminate subjected to loading are expressed as a function of the midplane displacements u_0 and v_0, respectively:

$$\begin{bmatrix} \varepsilon_{xx}^{0} \\ \varepsilon_{yy}^{0} \\ \gamma_{xy}^{0} \end{bmatrix} = \begin{bmatrix} \dfrac{\partial u_0}{\partial x} \\ \dfrac{\partial v_0}{\partial y} \\ \dfrac{\partial u_0}{\partial y} + \dfrac{\partial v_0}{\partial x} \end{bmatrix} \tag{2.4}$$

and

$$\begin{bmatrix} \kappa_{xx} \\ \kappa_{yy} \\ \kappa_{xy} \end{bmatrix} = \begin{bmatrix} \dfrac{\partial^2 w_0}{\partial x^2} \\ \dfrac{\partial^2 w_0}{\partial y^2} \\ 2\dfrac{\partial^2 w_0}{\partial x \partial y} \end{bmatrix} \tag{2.5}$$

And thermal and hygral strains are as follows:

$$\begin{bmatrix} \varepsilon_{xx}{}^{T} \\ \varepsilon_{yy}{}^{T} \\ \gamma_{xy}{}^{T} \end{bmatrix} = \begin{bmatrix} \alpha_{xx} \\ \alpha_{yy} \\ \alpha_{xy} \end{bmatrix} \Delta T \tag{2.6}$$

$$\begin{bmatrix} \varepsilon_{xx}{}^{H} \\ \varepsilon_{yy}{}^{H} \\ \gamma_{xy}{}^{H} \end{bmatrix} = \begin{bmatrix} \beta_{xx} \\ \beta_{yy} \\ \beta_{xy} \end{bmatrix} \Delta C \tag{2.7}$$

where

$$\begin{bmatrix} \alpha_{xx} \\ \alpha_{yy} \\ \alpha_{xy} \end{bmatrix} = \begin{bmatrix} \varepsilon_{xx}{}^{0} \\ \varepsilon_{yy}{}^{0} \\ \gamma_{xy}{}^{0} \end{bmatrix} \begin{matrix} \Delta C = 0 \\ \Delta T = 1 \end{matrix} \quad \text{and} \quad \begin{bmatrix} \beta_{xx} \\ \beta_{yy} \\ \beta_{xy} \end{bmatrix} = \begin{bmatrix} \varepsilon_{xx}{}^{0} \\ \varepsilon_{yy}{}^{0} \\ \gamma_{xy}{}^{0} \end{bmatrix} \begin{matrix} \Delta C = 1 \\ \Delta T = 0 \end{matrix}$$

After determining the strain field, the stress-strain relation for kth layer of composite plate (Fig. 2.3) based on the classical lamination theory can be written in the following form:

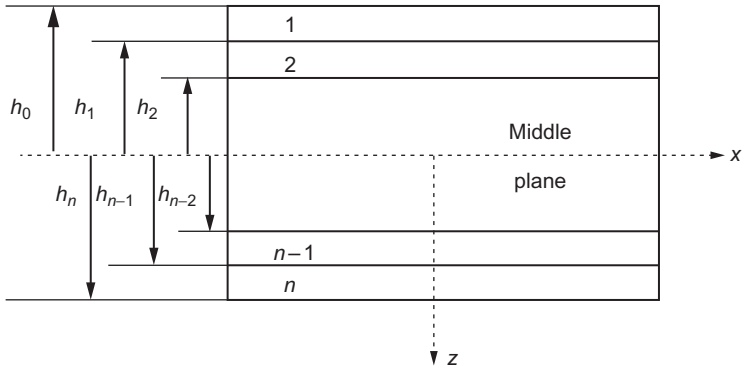

Fig. 2.3 Laminate convention [2].

$$\begin{bmatrix}\sigma_{xx}{}^{M}\\ \sigma_{yy}{}^{M}\\ \sigma_{xy}{}^{M}\end{bmatrix}_k = \begin{bmatrix}\bar{Q}_{11} & \bar{Q}_{12} & \bar{Q}_{16}\\ \bar{Q}_{12} & \bar{Q}_{22} & \bar{Q}_{26}\\ \bar{Q}_{16} & \bar{Q}_{26} & \bar{Q}_{66}\end{bmatrix}_k \begin{bmatrix}\varepsilon_{xx}\\ \varepsilon_{yy}\\ \gamma_{xy}\end{bmatrix} - \begin{bmatrix}\varepsilon_{xx}{}^{T}\\ \varepsilon_{yy}{}^{T}\\ \gamma_{xy}{}^{T}\end{bmatrix}_k - \begin{bmatrix}\varepsilon_{xx}{}^{H}\\ \varepsilon_{yy}{}^{H}\\ \gamma_{xy}{}^{H}\end{bmatrix}_k \tag{2.8}$$

where $\left[\bar{Q}_{ij}\right]_k$ are the elements of the transformed reduced stiffness matrix, determined as

$$\begin{aligned}
\bar{Q}_{11} &= Q_{11}cos^4\theta + 2(Q_{12}+2Q_{66})sin^2\theta cos^2\theta + Q_{22}sin^4\theta\\
\bar{Q}_{12} &= (Q_{11}+Q_{22}-4Q_{66})sin^2\theta cos^2\theta + Q_{12}\left(sin^4\theta + cos^2\theta\right)\\
\bar{Q}_{22} &= Q_{11}sin^4\theta + 2(Q_{12}+2Q_{66})sin^2\theta cos^2\theta + Q_{22}cos^4\theta\\
\bar{Q}_{16} &= (Q_{11}-Q_{12}-2Q_{66})sin\,\theta cos^3\theta + (Q_{12}-Q_{22}-2Q_{66})sin^3\theta cos\,\theta\\
\bar{Q}_{26} &= (Q_{11}-Q_{12}-2Q_{66})sin^3\theta cos\,\theta + (Q_{12}-Q_{22}+2Q_{66})sin\,\theta cos^3\theta\\
\bar{Q}_{66} &= (Q_{11}+Q_{22}-2Q_{12}-2Q_{66})sin^2\theta cos^2\theta + Q_{66}\left(sin^4\theta + cos^2\theta\right)
\end{aligned} \tag{2.9}$$

where the stiffness coefficients Q_{ij} that are related to the engineering constants are given as follows:

$$Q_{11} = \frac{E_1}{1-v_{21}v_{12}} \quad Q_{12} = \frac{v_{12}E_2}{1-v_{21}v_{12}} \quad Q_{22} = \frac{E_2}{1-v_{21}v_{12}} \quad Q_{66} = G_{12} \tag{2.10}$$

Here, E_1 and E_2, G_{12} are the longitudinal and transverse elastic modulus and in-plane shear modulus, respectively; v_{12} and v_{21} are major and minor Poisson's ratios.

For thin composite subjected to hygro-thermo-mechanical loading, in general, in-plane force resultants (force per unit width) and moment resultants (moment per unit width) have the following relations:

Force resultants:

$$\begin{bmatrix}N_x^M\\ N_y^M\\ N_x^M\end{bmatrix} = \begin{bmatrix}A_{11} & A_{12} & A_{16}\\ A_{12} & A_{22} & A_{26}\\ A_{16} & A_{26} & A_{66}\end{bmatrix} \begin{bmatrix}\varepsilon_{xx}{}^{0}\\ \varepsilon_{yy}{}^{0}\\ \gamma_{xy}{}^{0}\end{bmatrix} + \begin{bmatrix}B_{11} & B_{12} & B_{16}\\ B_{12} & B_{22} & B_{26}\\ B_{16} & B_{26} & B_{66}\end{bmatrix} \begin{bmatrix}k_{xx}\\ k_{yy}\\ k_{xy}\end{bmatrix} - \begin{bmatrix}N_x^T\\ N_y^T\\ N_{xy}^T\end{bmatrix} - \begin{bmatrix}N_x^C\\ N_y^C\\ N_{xy}^C\end{bmatrix} \tag{2.11}$$

The matrices [A] and [B] appearing in Eq. (2.11) can be defined as

$$A_{ij} = \sum_{k=1}^{N}\left[\bar{Q}_{ij}\right]_k(h_k - h_{k-1}) \quad (\text{Extensional stiffness}) \tag{2.12}$$

$$B_{ij} = \frac{1}{2}\sum_{k=1}^{N}\left[\bar{Q}_{ij}\right]_k\left(h_k^2 - h_{k-1}^2\right) \,(\text{Coupling stiffness})\,(i,j=1,2,6) \tag{2.13}$$

And $[N^T]$, and $[N^C]$ are the resultant thermal and hygral forces, respectively:

$$\begin{bmatrix} N_x^T \\ N_y^T \\ N_{xy}^T \end{bmatrix} = \Delta T \sum_{k=1}^{n} \begin{bmatrix} \bar{Q}_{11} & \bar{Q}_{12} & \bar{Q}_{16} \\ \bar{Q}_{12} & \bar{Q}_{22} & \bar{Q}_{26} \\ \bar{Q}_{16} & \bar{Q}_{26} & \bar{Q}_{66} \end{bmatrix}_k \begin{bmatrix} \alpha_x \\ \alpha_y \\ \alpha_{xy} \end{bmatrix}_k (h_k - h_{k-1}) \tag{2.14}$$

$$\begin{bmatrix} N_x^C \\ N_y^C \\ N_{xy}^C \end{bmatrix} = \Delta C \sum_{k=1}^{n} \begin{bmatrix} \bar{Q}_{11} & \bar{Q}_{12} & \bar{Q}_{16} \\ \bar{Q}_{12} & \bar{Q}_{22} & \bar{Q}_{26} \\ \bar{Q}_{16} & \bar{Q}_{26} & \bar{Q}_{66} \end{bmatrix}_k \begin{bmatrix} \beta_x \\ \beta_y \\ \beta_{xy} \end{bmatrix}_k (h_k - h_{k-1}) \tag{2.15}$$

Moment resultants:

$$\begin{bmatrix} M_x^M \\ M_y^M \\ M_{xy}^M \end{bmatrix} = \begin{bmatrix} \mathrm{B}_{11} & \mathrm{B}_{12} & \mathrm{B}_{16} \\ \mathrm{B}_{12} & \mathrm{B}_{22} & \mathrm{B}_{26} \\ \mathrm{B}_{16} & \mathrm{B}_{26} & \mathrm{B}_{66} \end{bmatrix} \begin{bmatrix} {\varepsilon_{xx}}^0 \\ {\varepsilon_{yy}}^0 \\ {\gamma_{xy}}^0 \end{bmatrix} + \begin{bmatrix} \mathrm{D}_{11} & \mathrm{D}_{12} & \mathrm{D}_{16} \\ \mathrm{D}_{12} & \mathrm{D}_{22} & \mathrm{D}_{26} \\ \mathrm{D}_{16} & \mathrm{D}_{26} & \mathrm{D}_{66} \end{bmatrix} \begin{bmatrix} k_{xx} \\ k_{yy} \\ k_{xy} \end{bmatrix} - \begin{bmatrix} M_x^T \\ M_y^T \\ M_{xy}^T \end{bmatrix} - \begin{bmatrix} M_x^C \\ M_y^C \\ M_{xy}^C \end{bmatrix} \tag{2.16}$$

where D_{ij} the bending stiffnesses, which are defined as in terms of lamina stiffness $\bar{Q}_{ij}$ as

$$D_{ij} = \frac{1}{3} \sum_{k=1}^{N} \left[\bar{Q}_{ij}\right]_k \left(h_k^3 - h_{k-1}^3\right) \tag{2.17}$$

In a more general representation, the constitutive equation of a laminated plate is obtained by grouping Eqs. (2.11) and (2.16) into a single-matrix equation of the form:

$$\begin{bmatrix} N_x \\ N_y \\ N_{xy} \\ M_x \\ M_y \\ M_{xy} \end{bmatrix} = \begin{bmatrix} A_{11} & A_{12} & A_{16} & \mathrm{B}_{11} & \mathrm{B}_{12} & \mathrm{B}_{16} \\ A_{12} & A_{22} & A_{26} & \mathrm{B}_{12} & \mathrm{B}_{22} & \mathrm{B}_{26} \\ A_{16} & A_{26} & A_{66} & \mathrm{B}_{16} & \mathrm{B}_{26} & \mathrm{B}_{66} \\ \mathrm{B}_{11} & \mathrm{B}_{12} & \mathrm{B}_{16} & \mathrm{D}_{11} & \mathrm{D}_{12} & \mathrm{D}_{16} \\ \mathrm{B}_{12} & \mathrm{B}_{22} & \mathrm{B}_{26} & \mathrm{D}_{12} & \mathrm{D}_{22} & \mathrm{D}_{26} \\ \mathrm{B}_{16} & \mathrm{B}_{26} & \mathrm{B}_{66} & \mathrm{D}_{16} & \mathrm{D}_{26} & \mathrm{D}_{66} \end{bmatrix} \begin{bmatrix} {\varepsilon_{xx}}^0 \\ {\varepsilon_{yy}}^0 \\ {\gamma_{xy}}^0 \\ k_{xx} \\ k_{yy} \\ k_{xy} \end{bmatrix} \tag{2.18}$$

The matrix given above is called as the stiffness matrix of the laminate. Here, the matrix B represents a coupling between stretching and bending of a laminate. In case the laminate is symmetrical, a stretching-bending coupling effect does not exist. Thus, the analyzing of the behavior of symmetrical matrices is much simpler than that of the laminates having a coupling effect.

2.2.2 Micromechanical analysis

In the macromechanical analysis discussed above, basic lamina constants E_1, E_2, G_{12}, and v_{12} are assumed to be known from direct experimental characterization of the unidirectional material. It is desirable to have reliable predictions of lamina constants as a function of constituent properties (matrix and fiber properties). A specialized area of composites involving a study of the interaction of constituent materials on the microscopic level is generally conducted by the use of a mathematical model describing the response of each constituent material. In this section, mechanics of material approach that the fibers and matrix are assumed to be under uniform stress is handled and the expressions are given for determination of the basic elastic properties of the lamina [5,6].

The longitudinal and transverse modulus, Poisson's ratio, and shear modulus are given, respectively, by the following relations:

$$E_1 = V_f E_{1f} + V_m E_m \tag{2.19}$$

$$E_2 = \frac{E_{2f} E_m}{V_f E_m + V_m E_{2f}} \tag{2.20}$$

$$v_{12} = V_f v_{12f} + V_m v_m \tag{2.21}$$

$$G_{12} = \frac{G_{12f} G_m}{V_f G_m + V_m G_{12f}} \tag{2.22}$$

where subscript 1 and 2 and f and m appearing in the above equations denote the longitudinal and transverse directions and fiber and matrix properties, respectively. V_f and V_m represent fiber and matrix volume fractions, respectively. In the above formulations, fibers are assumed to be transversely isotropic.

2.3 Mechanics of short fiber-reinforced composites

A number of models have been proposed to predict the physical properties of short-fiber and particulate-reinforced composites. These composite models can be grouped into five basic models: law of mixtures, shear lag, laminated plate, variational principle, and Eshelby's models. Law of mixtures and shear-lag models give poor estimation of stiffness of a composite where the aspect ratio of short fibers is small [7]. In addition, semiempirical models distinguish spherical and nonspherical particulate systems. These expressions are generally based on some physics arguments and determination of fitting parameters. Some semiempirical models that rely on the determination of adjustable parameters have been developed due to the complexity of the geometric features (filler aspect ratio, volume fraction, filler orientation, etc.) and inadequacies of the theoretical models.

2.3.1 Law of mixtures

It is considered that a composite with N different reinforcing elements is distributed in a matrix. Assume that each fiber has a shear modulus μ_i and volume fraction of fibers is V_i ($i = 1,2,3,\ldots,N$) and the shear modulus and volume fraction of matrix material are μ_0 and V_0, respectively. The shear modulus of composites μ_c is

$$\mu_c = \sum\nolimits_{i=0}^{N} V_i \mu_i \tag{2.23}$$

where

$$\sum\nolimits_{i=0}^{N} V_i = 1 \tag{2.24}$$

Assume that the externally applied shear strain γ_a is equal to shear strains in all phases including the matrix that can be explained as the average strain γ. Since the stress in the ith phase, σ_i, is given by $\mu_i\overline{\gamma}$, the average stress in the composite can be approached by

$$\overline{\sigma} = \sum_{i=0}^{N} V_i \sigma_i = \sum_{i=0}^{N} V_i \mu_i \overline{\gamma} \tag{2.25}$$

On the other hand, the average stress $\overline{\sigma}$ is related to the applied strain γ_a ($=\overline{\gamma}$) by

$$\overline{\sigma} = \mu_c \overline{\gamma} \tag{2.26}$$

If the shear moduli μ_c and μ_i are replaced by the strength of composite σ_c and reinforcing material σ_i, composite strength can be obtained as

$$\sigma_c = \sum\nolimits_{i=0}^{N} V_i \sigma_i \tag{2.27}$$

In the case of two-phase system, matrix, and one kind of reinforced element, Eq. (2.27) can be written as

$$\sigma_c = V_0\sigma_0 + V_1\sigma_1 = V_m\sigma_m + V_f\sigma_f \tag{2.28}$$

where the indexes m and f define matrix and fiber, respectively. The value predicted by law of mixtures is an upper bound, because the strain in the fiber and the matrix are not equal [7,8].

2.3.2 Shear lag model

Shear-lag model was developed by Cox [9] and adequately predicts the stress transfer in fiber-reinforced composites, particularly for large differences in inclusion to matrix elastic modulus ratios [10]. It is assumed that short fibers having uniform length and

diameter are aligned in the loading direction and distributed uniformly throughout the material as seen in Fig. 2.4A. A unit cell shown in Fig. 2.4B represents the basic model, in which short fiber surrounded by matrix. The other boundary of the surrounding matrix is taken as midsurface between two short fibers. This short-fiber composite is subjected to the applied uniaxial strain e along the z direction. Let the axial displacements in the fiber and the matrix on the boundary of the unit cell ($r = D/2$) be denoted by u and v, respectively.

In addition, it is assumed that the difference in the axial displacements, *u and v*, is proportional to the shear stress τ_0 at the matrix-fiber interface. One can obtain

$$\frac{d\sigma_f}{dz} = -\frac{4\tau_0}{d} = h(u - v) \tag{2.29}$$

where σ_f is the axial stress in the fiber. The first equality in Eq. (2.29) was derived by considering the equilibrium of force along the z direction. It is noted that the positive direction of shear stress τ_0 is taken through the positive z axis. In this step, Hooke's law is also valid for the fiber as

$$\sigma_f = E_f \frac{du}{dz} \tag{2.30}$$

Micromechanics is concerned with the prediction of elastic, viscoelastic, and strength properties of composites form those of their individual constituents. The objective of any such analysis is to model a heterogeneous material by an anisotropic continuum. The stresses and strains obtained by continuum analyzes are to be considered as

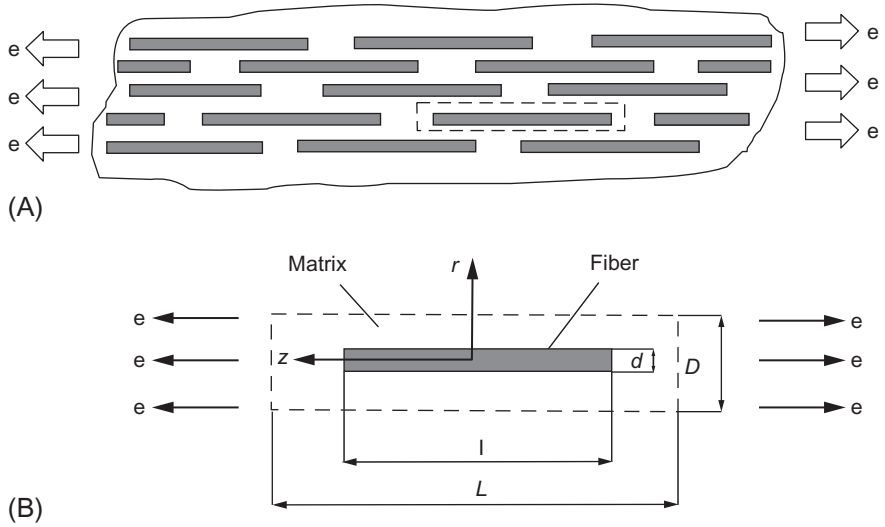

Fig. 2.4 Shear-lag model for aligned short-fiber composite: (A) representative short fiber and (B) unit cell model for shear-lag analysis [7].

averages over the smallest repetitive cell and are sufficiently accurate when changes in applied stresses are smaller distances of the size of the inclusions [8]. Micromechanics is still an area of active research in order to bring theoretical predictions into better agreement with experimental results. Reviews of earlier work pertaining to composites with continuous-fiber reinforcement can be found in textbooks [11,12] and review articles [13]. The various approaches proposed can be classified as follows: netting analysis, mechanics of materials, self-consistent model, variational, exact, statistical, discrete element, semiempirical methods, and microstructural theories. The usefulness of these theories lies in the fact that they provide some insight into the mechanics of fiber or particular application by the compounder and the stress analyst.

Most theories consider spherical, disk-shaped, or short-fiber isotropic inclusions in an isotropic matrix. Even though some fibers, such as Kevlar, are known to have a microfibrillar structure and are themselves anisotropic, the effective moduli predicted are in reasonable agreement with experimental results. The basic assumptions common to these analyzes are the following:

- The filler particles are of idealized shape (spherical, cubic, and rod-like).
- There is complete adhesion between matrix and filler.
- Elongations are small.
- Complete dispersion is achieved.
- Volume loadings are low enough to ignore interactions of order higher than two.
- The matrix can be considered to be continuous and homogeneous.

There are many examples of analytic and numerical modeling for microsized composites. However, in nanocomposite systems, several issues need to be developed. Some authors studying composite materials are generally interested in either prediction of elastic properties of the composite or volume-change problems.

Semiempirical models are most widely used expressions in the prediction of elastic modulus. These expressions are generally based on some physics arguments and determination of fitting parameters [14]. A better understanding of the mechanical behavior and predicted elastic modulus is essential in the development of the composites. This also assists the improvement of material processing. For this reason, the modulus of polymer composites has been extensively studied experimentally and predicted with a two-phase model by various researchers. Some semiempirical models that rely on the determination of adjustable parameters have been developed due to the complexity of the geometric features (filler aspect ratio, volume fraction, filler orientation, etc.) and inadequacies of the theoretical models as mentioned above. All of the theoretical modeling approaches based on the relations of the elastic constants are given in Eqs. (2.31a)–(2.31c). For an isotropic material, there are two elastic constants: Young's modulus (E) and Poisson's ratio (ν) to define the elastic response of the composites:

$$G = \frac{E}{2(1+\nu)} \tag{2.31a}$$

$$E = \frac{9KG}{3K+G} \tag{2.31b}$$

$$\nu = \frac{3K - 2G}{2(3K + G)} \tag{2.31c}$$

In the above equations, K refers to the bulk modulus, and G is shear modulus of the material. In the following section, semiempirical models for spherical and non-spherical particulate systems are investigated.

2.3.3 Semi empirical models for spherical particulate systems

Semiempirical models based on the physical parameters have the following general form [15]:

$$P_c = \frac{P_m\left(1 + \xi X V_f\right)}{1 - X\psi V_f} \tag{2.32a}$$

$$X = \frac{P_f - P_m}{P_f + xP_m} \tag{2.32b}$$

Here, P denotes the bulk modulus (K) or the shear modulus (G), and V_f is the volume fraction. The subscripts c, m, and f refer to the composite, matrix, and the filler, respectively. In this formulation, ξ and ψ can be treated as adjustable parameters that are specifically defined in each model. Based on the formulation given in Eqs. (2.32a), (2.32b), there are several formulations proposed in the literature in order to predict the elastic modulus of the composites reinforced by spherical fillers. In these systems, the reinforcing particles are considered to be spherical or near spherical; therefore, the effective aspect ratio is unity. The following four most commonly used models were developed by Guth and Gold, Halpin-Tsai (HT), Lewis-Nielsen (LN), and Chantler, Hu, and Boyd (Ch) that are related with the adjustable parameters ξ and ψ.

2.3.3.1 Halpin-Tsai model

Halpin and Tsai developed a widely used composite theory to predict the stiffness of continuous-fiber composites as a function of aspect ratio. This theory is based on the early micromechanical work of Hermans [16] and Hill [17]. Halpin and Tsai adapted Hermans' model for particulate systems. Based on Eq. (2.32), P represents the Young's modulus, ξ is a shape parameter that depends on matrix Poisson's ratio, filler geometry, orientation, and loading direction, and it was found to be 2 for particulate-filled composites. Moreover, for shear-modulus predictions, $\xi = 1$ can be used or the equality as follows:

$$\xi_G = \frac{7 - 5\nu_m}{8 - 10\nu_m} \tag{2.33a}$$

By including matrix Poisson's ratio (ν_m), the parameter can be calculated precisely. In the same manner for bulk modulus, the term is as follows:

$$\xi_K = \frac{2(1-2\nu_m)}{1+\nu_m} \tag{2.33b}$$

The last parameter, ψ, used in Eqs. (2.32a), (2.32b) is taken as 1 in Halpin-Tsai model. The Halpin-Tsai equations are known to fit some experimental data very well at low volume fractions, but it underestimates stiffness values at high volume fractions [18]. This has prompted some modifications to their model. By adapting this formulation to the short-fiber composites, Halpin and Tsai noted that the shape parameter, ξ, lies between 0 and ∞. For example, if ξ is taken as ∞, then Eqs. (2.32a), (2.32b) reduced to the rule of mixtures as in the following form [19]:

$$P = \nu_f P_f + \nu_m P_m \tag{2.34a}$$

However, for $\xi = 0$, Halphin-Tsai formulation becomes the inverse rule of mixture as follows:

$$\frac{1}{P} = \frac{\nu_f}{P_f} + \frac{\nu_m}{P_m} \tag{2.34b}$$

2.3.3.2 Lewis-Nielsen model

This model was developed by Nielsen [20] and Lewis and Nielsen [21] using the analogy between the stiffness of the composite and viscosity of a suspension of rigid particle in a Newtonian fluid. This model is also a modification of the Halpin-Tsai model. It was designed to compensate the Halpin-Tsai model's lack for the prediction of modulus at high-filler-loading composites. In their formulation, an equation in which the stiffness not only matches with dilute theory at low volume fractions but also displays rigid reinforcement as V_f approaches a packing limit ${V_f}^{\max}$. It is used to account for the limits imposed by the maximum packing for uniformly sized spherical particles. The following expressions are given for the model:

$$\xi_G = \frac{7-5\nu_m}{8-10\nu_m} \tag{2.35a}$$

$$\xi_K = \frac{2(1-2\nu_m)}{1+\nu_m} \tag{2.35b}$$

$$\psi = 1 + \left(\frac{1-{V_f}^{\max}}{\left({V_f}^{\max}\right)^2}\right) V_f \tag{2.35c}$$

Here, v_m is matrix Poisson's ratio and ${V_f}^{\max}$ is the maximum volume fraction of filler. For uniform sizes of spheres, ${V_f}^{\max}$ is 0.66 for random packing, and if the composite system does not have uniform size distribution of particles, then ${V_f}^{\max}$ is considered to

be between 0.66 and 1 [14]. The parameters, ξ_G and ξ_K, are used for the prediction of shear and bulk modulus, respectively. It is obvious that ξ_G and ξ_K are the same as in Halpin-Tsai model; however, the parameter ψ is a function of volume fraction and maximum volume fraction of the filler in the Lewis-Nielsen model.

2.3.3.3 S-combining rule

This approach considers a composite system with the stiff spherical inclusions in a more compliant matrix, such that for particulate-filled polymers with $P_f > P_m$. For rigid uniformly sizes of spheres, the adjustable parameters ξ_G, ξ_K, and ψ can be expressed as follows [18]:

$$\xi_G = \frac{7 - 5\nu_m}{8 - 10\nu_m} \tag{2.36a}$$

$$\xi_K = \frac{2(1 - 2\nu_m)}{1 + \nu_m} \tag{2.36b}$$

$$\psi = 1 + \left(\frac{1 - {V_f}^{\max}}{{V_f}^{\max}}\right)\left(V_f.{V_f}^{\max} + \left(1 + V_f\right)\left(1 - {V_f}^{\max}\right)\right) \tag{2.36c}$$

Here, ${V_f}^{\max}$ is the maximum volume fraction of the filler. Comparing the Halpin-Tsai, Lewis-Nilsen, and S-combining rule, it can be seen that the parameter ψ has different mathematical form in each model. Therefore, it can be useful to investigate the variation of ψ for appropriate maximum volume fraction of filler and V_f. Fig. 2.5 shows this effect for different values of ${V_f}^{\max}$. Another important difference among HT, LN, and S-combining rule models is that Young's modulus values may not be predicted directly by LN or S-combining models, while HT model allows prediction of Young's modulus of the composite without extra calculation. Young's modulus can be generated from the predicted values of bulk modulus K and shear modulus G through the auxiliary expression given in Eqs. (2.31a)–(2.31c) for LN or S-combining models.

2.3.3.4 Chantler, Hu, and Boyd (CHU) model

Chantler and coworkers presented a new phenomenological model based on the classic Hertzian elastic contact theory. The following expression can be used to predict the elastic modulus of composites (E_c) [22]:

$$E_c = E_m\left(E_f/E_m\right)^{1-\left(1-V_f\right)^{\beta}} \tag{2.37a}$$

where

$$\beta = \frac{2\left[\left(1 - \nu_f^2\right)/\left(1 - \nu_m^2\right)\right]^{1.7}}{ln\left(E_f/E_m\right)} \tag{2.37b}$$

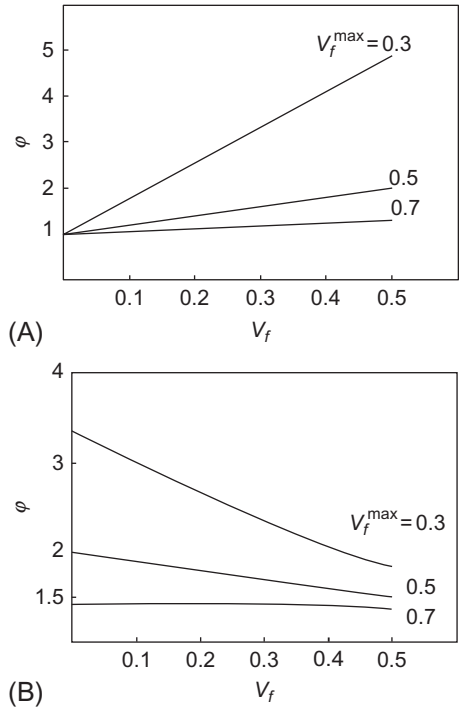

Fig. 2.5 Effect of adjustable parameter ψ for (A) Lewis-Nilsen model and (B) S-combining rule with different values of $V_f{}^{max}$.

where v_f and v_m are Poisson's ratio of the filler and matrix and E_m and E_f are the elastic modulus of matrix and filler, respectively. The results of this study demonstrate that the previous phenomenological model given in Braem et al. [23] is deficient if the modulus ratio E_f/E_m is higher than 10. A modified approach gives much improved predictions for composite modulus and also satisfies the boundary conditions for bulk filler and resin materials. In contrast to the previously mentioned models (HT, LN, and S), CHB model considers Poisson's ratio of the filler (v_f). However, the reported studies about the nanocomposite modeling indicate that the effective material parameter is only v_m. As in HT model, CHB model also allows calculation of Young's modulus directly.

2.3.3.5 Guth and Gold model

By adapting the Einstein coefficient, (K_E) is equal to 2.5 in the Einstein equation, which is valid only at very low concentrations (< %10) of the filler, Guth and Gold [24] obtained the following formulation that is only applicable to elastomers filled with a certain amount of spherical fillers, and the formulation can be used for concentrations up to 30%:

$$E_c = E_m\left[1 + 2.5V_f + 14.1V_f{}^2\right] \tag{2.38a}$$

Most of the models adequately predict the behavior for particulate-filled systems in the volume-fraction concentration in the range of $0 \leq V_f \leq 1/3$; however, only S-combining rule and Lewis-Nielsen models have the capability of prediction at higher volume-fraction concentrations of filler [18]. To increase the capability of prediction of Guth and Gold model at higher volume fraction, the equation is modified in the following form, which is valid at filler concentration of up to 45%:

$$E_c = E_m\left[1 + 2.5V_f + 16.2{V_f}^2\right] \tag{2.38b}$$

2.3.4 Semi empirical models for nonspherical particulate systems

The composite systems such as in layered clay/polymer nanocomposites contain platelet like nonspherical particles. Nonspherical particulate-reinforced composites have slightly higher elastic modulus (E) than those based on spherical particulate systems. There are several important models that have appropriate prediction capability of elastic modulus of the nonspherical filled composite systems. In this section, we consider four different models developed for the estimation of elastic modulus of inorganic clay-layer-incorporated thermoset polymer nanocomposites.

2.3.4.1 Halpin-Tsai model

Halpin-Tsai equations are widely used expressions in order to predict reinforcement effect of fillers in nanocomposite systems with both spherical (or near spherical) and nonspherical filled systems. Halpin-Tsai equations were modified by Halpin and Kardos [19] for the plate-like filler as expressed in the following form:

$$E_c = \frac{E_m\left(1 + \xi\eta V_f\right)}{1 - \eta V_f} \tag{2.39a}$$

where

$$\eta = \frac{E_f/E_m - 1}{E_f/E_m + \xi} \tag{2.39b}$$

Here, E_f denotes elastic modulus of the filler, and ξ is the shape factor depending on the filler orientation and loading direction. For the rectangular plate-like filler in a composite system, ξ is equal to $2w/t$ in which w is the width and t is the thickness of the dispersed phase. The effect of aspect ratio on Halpin-Tsai model is illustrated in Fig. 2.6. The aspect ratio α has very significant effect on elastic modulus of the composite even at low volume fraction of the filler.

2.3.4.2 Modified Halpin-Tsai model

Lewis and Nielsen [21] and Nielsen [20] considered the maximum volumetric packing fraction of the filler ψ as an additional parameter in order to improve the prediction ability of the classical HT model. Maximum volumetric packing fraction can be

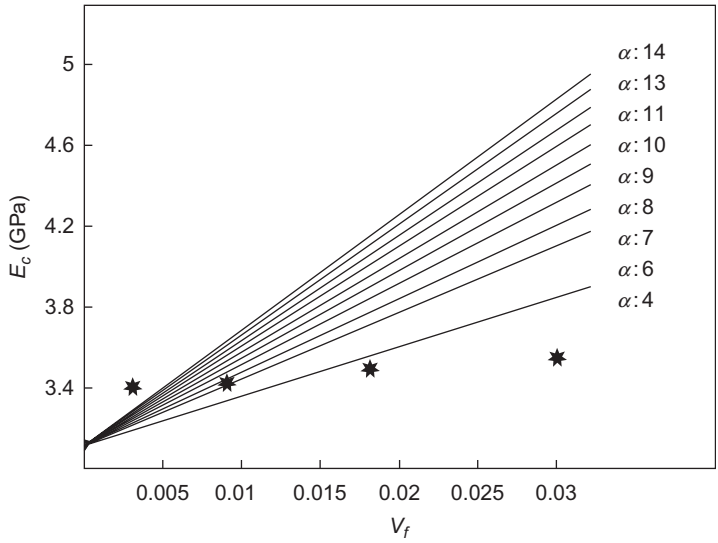

Fig. 2.6 Effect of the aspect ratio, α, on the elastic modulus of the composite reinforced by nonspherical particulate fillers based on Halpin-Tsai equation (experimental data for MMT/epoxy are presented with (✸)).

defined as the ratio of true volume of the filler to apparent volume occupied by the filler. Modified Halpin-Tsai model can be written in the following form:

$$E_c = \frac{E_m\left(1+\xi\eta V_f\right)}{1-\psi\eta V_f} \tag{2.40a}$$

where

$$\psi = 1+\left(\frac{1-{V_f}^{\max}}{\left({V_f}^{\max}\right)^2}\right)V_f \tag{2.40b}$$

$$\eta = \frac{E_f/E_m-1}{E_f/E_m+\xi} \tag{2.40c}$$

Based on Lewis and Nielsen [21] and Nielsen [20] modification, Fig. 2.7. shows the effect of the aspect ratio α on the elastic modulus of the composite reinforced by nonspherical particulate fillers based on modified Halpin-Tsai equation. Similar to Halpin-Tsai model for nonspherical systems, the modified Halpin-Tsai model predicts a significant effect of aspect ratios of filler on the modulus of the composite.

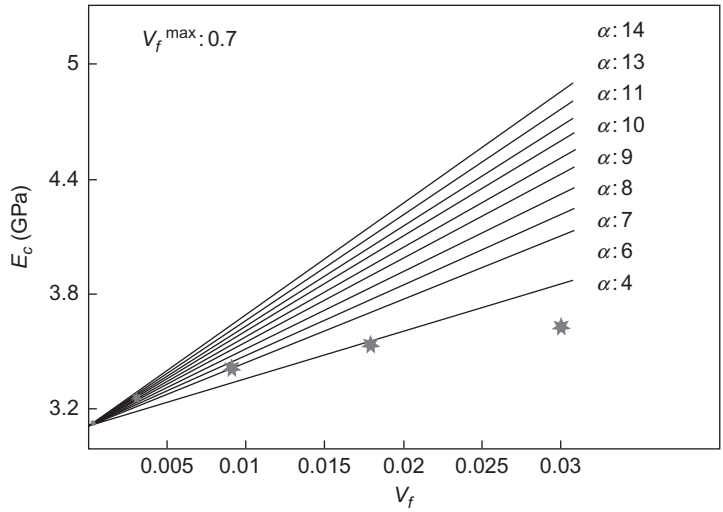

Fig. 2.7 Effect of the aspect ratio α on the elastic modulus of the composite reinforced by nonspherical particulate fillers based on modified Halpin-Tsai method for $V_f{}^{\max}=0.7$ (experimental data for OMMT/epoxy are presented with (✸)).

2.3.4.3 Guth model

The relations between Young's modulus and the concentration of filler given by Guth and Gold in Eqs. (2.38a), (2.38b) were modified by Guth [25] for nonspherical filled particulate composites. This modified model considers the chains composed of spherical fillers that are similar to rod-like filler particles embedded in a continuous matrix. By introducing a shape factor to original Guth and Gold equation, Guth developed a new expression as in the following form:

$$E_c = E_m\left[1+0.67\alpha V_f+1.62\left(\alpha V_f\right)^2\right] \tag{2.41}$$

where α is the shape factor (length/width of the filler), E_m is the elastic modulus of the matrix, and E_c is the elastic modulus of the composite [26].

2.3.4.4 Brodnyan model

Modifying the Mooney equation [27,28] expressed the following equation to predict the elastic modulus of the nonspherical particulate composites under the restriction of $1<\alpha<15$:

$$E_c = E_m\mathrm{Exp}\left(\frac{2.5V_f+0.407(\alpha-1)^{1.508}V_f}{1-V_f/V_f{}^{\max}}\right) \tag{2.42}$$

2.4 Mechanics of woven fabric composites

Orthogonal two-dimensional woven-fabric composites consist of threads such as strands, yarns, and woven rovings in warp direction L and weft (fill yarns) direction T that are principal directions. Woven have good stability in the warp and filling directions. Weaves repeat after a certain number of warp, weft strands, or yarns. Plain weave, 3×1 twill, cross ply weave, and unidirectional weave are some common weave styles. Weaves contain repetitive pattern in both directions as shown in Fig. 2.8. Some disadvantages of woven fabrics related to the design of certain composite products can be regarded as anisotropy, poor in-plane shear resistance, difficult handling of open constructions, and yarn-to-fabric tensile translation efficiency due to yarn crimp and crimp exchange [30].

Mechanical properties in plain-weave fabric become almost identical in two directions of warp and weft. However, the plain-weave fabric enables a high degree of crimp to the fibers, which decreases some mechanical performances of the composite. In twill-weave fabric, a regular diagonal pattern is produced on the cloth. The twill-weave cloth provides slippage that occurs between the fibers. In unidirectional-weave fabric, the threads are formed in the warp direction. The warp threads in the unidirectional weave are held together by fine weft threads. Maximum mechanical performance is obtained in the warp direction [4].

2.4.1 Constitutive equations

In mechanical analysis of the woven-fabric laminates, the elastic properties of warp and left unidirectional layers shown in Fig. 2.9 are used as in the following form:

$$\text{Warp layer}: \quad E_{Lwp}\ E_{Twp}\ v_{LTwp}\ G_{LTwp}$$

$$\text{Weft layer}: \quad E_{Lwf}\ E_{Twf}\ v_{LTwf}\ G_{LTwf}$$

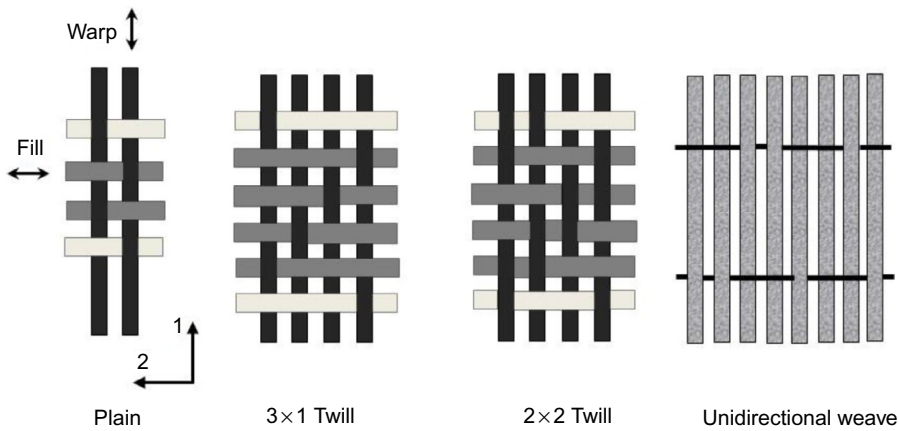

Fig. 2.8 Schematic representation of woven-fabric weave styles [29].

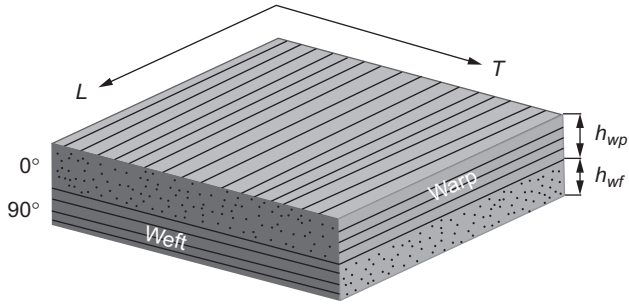

Fig. 2.9 Laminate analogy of a layer of reinforced cloth.

These elastic properties refer to the respective principal directions of each layer.

The reduced stiffness matrix coefficients of the warp layer with respect to the principal direction of the warp layer and thus reinforced cloth layer can be given from Eq. (2.10) as follows:

$$Q_{11}^{wp} = \alpha_{wp} E_{Lwp} \quad Q_{12}^{wp} = \alpha_{wp} \nu_{LTwp} E_{Lwp} \quad Q_{22}^{wp} = \alpha_{wp} E_{Twp} \tag{2.43}$$

$$Q_{16}^{wp} = Q_{26}^{wp} = 0 \quad Q_{66}^{wp} = G_{LTwp} \tag{2.44}$$

where

$$\alpha_{wp} = \frac{1}{1 - \dfrac{E_{Twp}}{E_{Lwp}} \nu_{LTwp}^2}$$

Similarly, the reduced stiffness matrix coefficients of the weft layer can be expressed in its principal directions as follows:

$$Q_{11}^{wf} = \alpha_{wf} E_{Lwf} \quad Q_{12}^{wf} = \alpha_{wf} \nu_{LTwf} E_{Twf} \quad Q_{22}^{wf} = \alpha_{wf} E_{Twf} \tag{2.45}$$

$$Q_{16}^{wf} = Q_{26}^{wf} = 0 \quad Q_{66}^{wf} = G_{LTwf} \tag{2.46}$$

where

$$\alpha_{wf} = \frac{1}{1 - \dfrac{E_{Twf}}{E_{Lwf}} \nu_{LTwf}^2}$$

The extension stiffness matrix coefficients A_{ij} $(i, j = 1, 2, 6)$ given by Eq. (2.12) that define the behavior of the cloth reinforcement layer can be expressed as

$$A_{ij} = h_{wp} Q_{ij}^{wp} + h_{wf} Q_{ij}^{wf} \tag{2.47}$$

where h_{wp} and h_{wf} are warp and weft layer thicknesses expressed as functions of the thickness e_c of the layer and of the balancing coefficient k along the warp in the following forms:

$$h_{wp} = ke_c \quad h_{wf} = (1-k)e_c \tag{2.48}$$

The cloth is specified as unidirectional in both warp and weft directions for $k=1$ and 0, respectively. The cloth is balanced for $k=1$.

The in-plane behavior of a cloth-reinforced layer is defined by the following constitutive equation:

$$\begin{bmatrix} N_x \\ N_y \\ N_{xy} \end{bmatrix} = \begin{bmatrix} A_{11} & A_{12} & 0 \\ A_{12} & A_{22} & 0 \\ 0 & 0 & A_{66} \end{bmatrix} \begin{bmatrix} \varepsilon_{xx}^0 \\ \varepsilon_{yy}^0 \\ \gamma_{xy}^0 \end{bmatrix} \tag{2.49}$$

For the case of tension in the warp direction, in-plane resultant forces are

$$N_x \neq 0, \quad N_y = 0, \quad N_{xy} = 0 \tag{2.50}$$

Then, $N_x = A_{11}\varepsilon_{xx}^0 + A_{12}\varepsilon_{yy}^0$, and hence

$$N_x = \left(A_{11} + \frac{A_{12}^2}{A_{22}}\right)\varepsilon_{xx}^0 \quad \text{can be obtained} \tag{2.51}$$

Elastic properties, the Young modulus, and Poisson's ratio in the weft direction are as following:

$$E_L = \frac{1}{e_c}\left(A_{11} - \frac{A_{12}^2}{A_{22}}\right) \tag{2.52}$$

$$v_{LT} = \frac{A_{12}}{A_{22}} \tag{2.53}$$

For the case of tension in the weft direction, Young's modulus E_T and the Poisson ratio v_{TL} are described, respectively as

$$E_T = \frac{1}{e_c}\left(A_{22} - \frac{A_{12}^2}{A_{11}}\right) \quad v_{TL} = \frac{A_{12}}{A_{11}} = v_{LT}\frac{E_T}{E_L} \tag{2.54}$$

For the case of in-plane shear in the weft direction, the shear modulus G_{LT} is defined as

$$G_{LT} = G_{TL} = \frac{1}{e_c}A_{66} \tag{2.55}$$

The elastic constants of a two-dimensional cloth-reinforced layer obtained by the equations given above can be written in the following form substituting the A_{ij} coefficients as

$$E_L = (1-\alpha)\left[k\alpha_{wp}E_{Lwp} + (1-k)\alpha_{wf}E_{Twf}\right] \tag{2.56}$$

$$E_T = (1-\alpha)\left[k\alpha_{wp}E_{Twp} + (1-k)\alpha_{wf}E_{Lwf}\right] \tag{2.57}$$

$$v_{LT} = \frac{k\alpha_{wp}v_{LTwp}E_{Twp} + (1-k)\alpha_{wf}v_{LTwf}E_{Twf}}{k\alpha_{wp}E_{Twp} + (1-k)\alpha_{wf}E_{Lwf}} \tag{2.58}$$

$$G_{LT} = kG_{LTwp} + (1-k)G_{LTwf} \tag{2.59}$$

where

$$\alpha = \frac{\left[k\alpha_{wp}v_{LTwp}E_{Twp} + (1-k)\alpha_{wf}v_{LTwf}E_{Twf}\right]^2}{\left[k\alpha_{wp}E_{Lwp} + (1-k)\alpha_{wf}E_{Twf}\right]\left[k\alpha_{wp}E_{Twp} + (1-k)\alpha_{wf}E_{Lwf}\right]} \tag{2.60}$$

The above expressions (Eqs. 2.56–2.59) can be simplified for various types of cloths by the value of the balancing coefficient k. For example, in the case where the fibers in the warp and weft directions are identical, the cloth is called balanced [29]. In fact, in this case, $k = 1/2$, and the moduli in warp and weft directions become identical:

$$E_{Lwp} = E_{Lwf} = E_{Lu} \tag{2.61}$$

$$E_{Twp} = E_{Twf} = E_{Tu} \tag{2.62}$$

$$v_{LTwp} = v_{LTwf} = v_{LTu} \tag{2.63}$$

$$G_{LTwp} = G_{LTwf} = G_{LTu} \tag{2.64}$$

where E_{Lu}, E_{Tu}, G_{LTu}, and v_{LTu} are the moduli of a unidirectional layer having a volume fraction equal to that of the reinforced cloth layer. In this regard, Eqs. (2.56)–(2.59) are expressed as follows:

$$E_L = E_T = (1-\alpha)\alpha_u(E_{Lu} + E_{Tu}) \tag{2.65}$$

$$v_{LT} = \frac{2v_{LT_u}}{1 + \dfrac{E_{Lu}}{E_{Tu}}} \tag{2.66}$$

$$G_{LT} = G_{LT_u} \tag{2.67}$$

where

$$\alpha_u = \frac{1}{1 - \dfrac{E_{Tu}}{E_{Lu}}v_{LT_u}^2}$$

2.5 Interface mechanics in fiber-reinforced composites

This section is mainly based on the study presented by Lei et al. [31]. Material's microstructure has an essential role in mechanical behavior of fiber-reinforced composites. As a microstructural entity, "interface" between fiber and matrix components has the responsibility to transfer load from matrix to fiber. However, there are various issues that may occur at the interface including interface debonding and damage. The quality of the interface has a significant effect on mechanical properties such as impact and fracture. Hence, it is important to investigate the behavior of the interface region and its effect on macrostructural properties.

The interface region may encounter several issues. These are interface intact bonding, interface debonding, interface completely debonding, and fiber pullout. During the debonding process, the interface properties continuously change. In order to analyze the interface, it is important to calculate the interfacial stresses. By using Cox's shear-lag model, it is possible to relate the fiber axial stress, σ, and the interfacial shear stress, τ, as

$$\tau = -\frac{r}{2}\left(\frac{d\sigma}{dx}\right) \tag{2.68}$$

Before interface debonding occurs, the fiber axial stress can be expressed by using Piggot's model as

$$\sigma = \sigma_{app}\frac{sinh\left[n(L-x)/r\right]}{sinh\left(ns\right)} \tag{2.69}$$

where x is the distance to the fiber entry, σ_{app} is the stress acting on the fiber out of the matrix, L is the effective length of the stress transfer, s is the fiber aspect ratio, and n is a constant, which depends on geometry and material properties of fiber and matrix.

By using Eqs. (2.68), (2.69), the interfacial shear stress along the fiber can be expressed as

$$\tau = \sigma_{app}\frac{ncosh\left[n(L-x)/r\right]}{sinh\left(ns\right)} \tag{2.70}$$

If a fiber pullout experiment is performed, the aspect ratio of the fiber is large. Therefore, fiber stress and shear stress at the fiber entry, that is, $x = 0$, can be calculated as

$$\sigma_m = \sigma \tag{2.71a}$$

$$\tau_m = \frac{n\sigma}{2} \tag{2.71b}$$

If the fiber stress exceeds the fiber strength σ_b, then fiber fracture can occur. On the other hand, if the interfacial shear stress exceeds the interfacial shear strength τ_b, then interface debonding can occur:

$$\sigma_m = \frac{2\tau_m}{n} \geq \sigma_b \quad \text{Fiber fracture} \tag{2.72a}$$

$$\tau_m = \frac{n\sigma}{2} \geq \tau_b \quad \text{Interface debonding} \tag{2.72b}$$

Moreover, if fiber strength is high and interfacial shear strength is low, then it is likely that interfacial debonding will occur as the damage mode.

2.6 Mechanics of curved composites

This section is mainly based on the study presented by Akbarov and Guz [32]. Curved composites are unidirectional fibrous and layered composites where fibers or layers are in the form of curvatures. These curvatures occur due to either design features or technological processes. If the curvatures are due to design features, then they can be modeled as periodical. However, if the curvatures are due to technological processes, then they are considered as local.

For simplicity, let us assume that curvatures only exist in Ox_1x_2 plane as shown in Fig. 2.10. The total thickness of N number of curved layers can be calculated as

$$\Delta H = h_1 + h_2 + \cdots + h_N \tag{2.73}$$

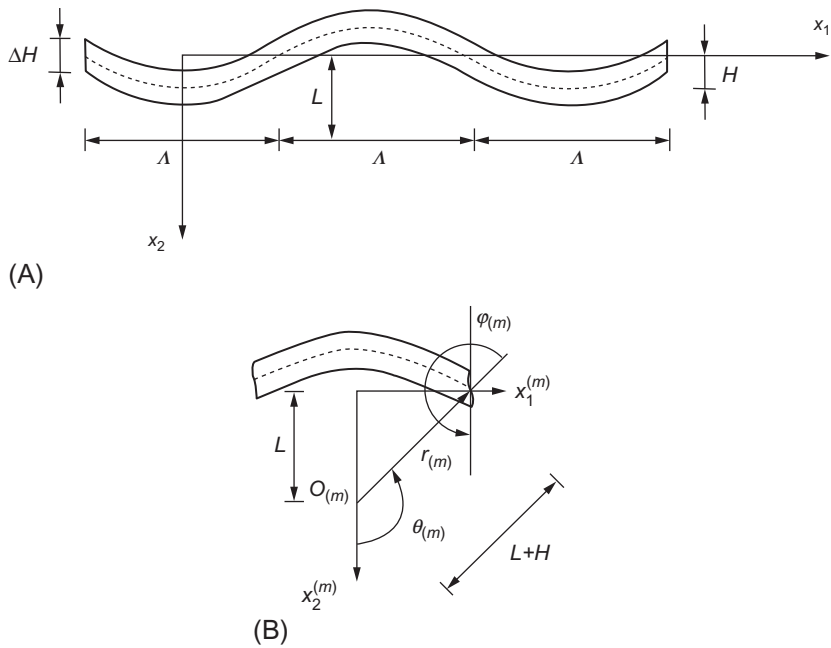

Fig. 2.10 (A) Representative layer and (B) approximation of the representative [32].

where h_i is the thickness of the ith layer. The maximum layer thickness is defined as

$$h' = \max\{h_1, h_2, \ldots, h_N\} \tag{2.74}$$

In Fig. 2.10, Λ is the half wavelength of the curvature, and H is the rise of the curve. It can be assumed that the composite material has a regular and periodic curvature with a period of 2Λ and following conditions should hold

$$h' \ll H, \quad \Delta H \ll \Lambda, \quad H \ll \Lambda, \quad \Lambda \ll L, \quad \Lambda \ll d \tag{2.75}$$

In order to obtain the constitutive relationships, Fig. 2.10A can be approximated as in Fig. 2.10B based on the inequalities given in Eq. (2.70). Note that a local coordinate system is introduced for each half period. For the mth half period, the local Cartesian coordinates are defined as

$$x_1^{(m)} = x_1 - (m-1)\Lambda, \quad x_2^{(m)} = x_2, \quad x_3^{(m)} = x_3 \quad -\infty \le m \le +\infty \tag{2.76}$$

The local Cartesian coordinate system can also be related to a local cylindrical coordinate system as

$$r_{(m)} cos\theta_{(m)} = x_2^{(m)} - (-1)^m L, \quad r_{(m)} sin\theta_{(m)} = x_1^{(m)}, \quad \varphi_{(m)} = 2\pi - \theta_{(m)} \tag{2.77}$$

For the mth half period, the stress-strain relationships in cylindrical coordinates can be written as

$$\sigma_{rr} = \overset{\circ}{A}_{11}\varepsilon_{rr} + \overset{\circ}{A}_{12}\varepsilon_{\theta\theta} + \overset{\circ}{A}_{13}\varepsilon_{33} \tag{2.78a}$$

$$\sigma_{\theta\theta} = \overset{\circ}{A}_{12}\varepsilon_{rr} + \overset{\circ}{A}_{22}\varepsilon_{\theta\theta} + \overset{\circ}{A}_{23}\varepsilon_{33} \tag{2.78b}$$

$$\sigma_{33} = \overset{\circ}{A}_{13}\varepsilon_{rr} + \overset{\circ}{A}_{23}\varepsilon_{\theta\theta} + \overset{\circ}{A}_{33}\varepsilon_{33} \tag{2.78c}$$

$$\sigma_{\theta 3} = 2\overset{\circ}{A}_{44}\varepsilon_{\theta 3} \tag{2.78d}$$

$$\sigma_{r3} = 2\overset{\circ}{A}_{55}\varepsilon_{r3} \tag{2.78e}$$

$$\sigma_{r\theta} = 2\overset{\circ}{A}_{66}\varepsilon_{r\theta} \tag{2.78f}$$

where $\overset{\circ}{A}_{ij}$ and $\overset{\circ}{G}_{ij}$ are effective (normalized) elastic constants and $\overset{\circ}{A}_{44} = \overset{\circ}{G}_{23}$, $\overset{\circ}{A}_{55} = \overset{\circ}{G}_{13}$, and $\overset{\circ}{A}_{66} = \overset{\circ}{G}_{12}$.

Based on the inequalities given in Eq. (2.75), a small parameter, ε, can be defined as

$$\varepsilon = \frac{\Lambda}{\pi L} \ll 1 \tag{2.79}$$

since

$$\Lambda^2 \approx 8LH \quad \text{and} \quad \varepsilon = \frac{\Lambda}{\pi L} \approx \frac{8H}{\pi \Lambda} \ll 1 \tag{2.80}$$

Hence, the stress-strain relationships given in Eqs. (2.78a)–(2.78f) can be written in Cartesian coordinates by using the parameter ε as

$$\sigma_{11} = A_{11}\varepsilon_{11} + A_{12}\varepsilon_{22} + A_{13}\varepsilon_{33} + 2A_{16}\varepsilon_{12} \tag{2.81a}$$

$$\sigma_{22} = A_{12}\varepsilon_{11} + A_{22}\varepsilon_{22} + A_{23}\varepsilon_{33} + 2A_{26}\varepsilon_{12} \tag{2.81b}$$

$$\sigma_{33} = A_{13}\varepsilon_{11} + A_{23}\varepsilon_{22} + A_{33}\varepsilon_{33} + 2A_{36}\varepsilon_{12} \tag{2.81c}$$

$$\sigma_{12} = A_{16}\varepsilon_{11} + A_{26}\varepsilon_{22} + A_{36}\varepsilon_{33} + 2A_{66}\varepsilon_{12} \tag{2.81d}$$

$$\sigma_{23} = 2A_{44}\varepsilon_{23} + 2A_{45}\varepsilon_{13} \tag{2.81e}$$

$$\sigma_{13} = 2A_{45}\varepsilon_{23} + 2A_{65}\varepsilon_{13} \tag{2.81f}$$

where

$$A_{11} = A_{11}^{\circ} + \varepsilon^2\left(-A_{11}^{\circ} + A_{12}^{\circ} + 2G_{12}^{\circ}\right)2sin^2\theta \tag{2.82a}$$

$$A_{12} = A_{12}^{\circ} + \varepsilon^2\left(A_{11}^{\circ} + A_{22}^{\circ} - 2A_{12}^{\circ} - 4G_{12}^{\circ}\right)sin^2\theta \tag{2.82b}$$

$$A_{23} = A_{23}^{\circ} + \varepsilon^2\left(A_{13}^{\circ} - A_{23}^{\circ}\right)sin^2\theta \tag{2.82c}$$

$$A_{16} = \varepsilon\left(-A_{11}^{\circ} + A_{12}^{\circ} + 2G_{12}^{\circ}\right)sin\theta \tag{2.82d}$$

$$A_{26} = \varepsilon\left(A_{11}^{\circ} - A_{12}^{\circ} - 2G_{12}^{\circ}\right)sin\theta \tag{2.82e}$$

$$A_{36} = \varepsilon\left(A_{23}^{\circ} - A_{13}^{\circ}\right)sin\theta \tag{2.82f}$$

$$A_{33} = A_{33}^{\circ} \tag{2.82g}$$

$$A_{22} = A_{22}^{\circ} + \varepsilon^2\left(-A_{22}^{\circ} + A_{12}^{\circ} + 2G_{12}^{\circ}\right)2sin^2\theta \tag{2.82h}$$

$$A_{13} = A_{13}^{\circ} + \varepsilon^2\left(A_{23}^{\circ} - A_{13}^{\circ}\right)sin^2\theta \tag{2.82i}$$

$$A_{44} = G_{23}^{\circ} + \varepsilon^2\left(G_{13}^{\circ} - G_{23}^{\circ}\right)sin^2\theta \tag{2.82j}$$

$$A_{66} = G_{12}^{\circ} + \varepsilon^2\left(A_{11}^{\circ} + A_{22}^{\circ} - 2A_{12}^{\circ} - 2G_{12}^{\circ}\right)sin^2\theta \tag{2.82k}$$

$$A_{45} = \varepsilon\left(G_{13}^{\circ} - G_{23}^{\circ}\right)sin\theta \tag{2.82l}$$

$$A_{55} = G_{13}^{\circ} + \varepsilon^2 \left(G_{23}^{\circ} - G_{13}^{\circ}\right) sin^2\theta \tag{2.82m}$$

and

$$\theta = \frac{\pi X_1}{\Lambda} \tag{2.83}$$

The formulation can be extended to 3D by considering the periodic curved structure. In this case, the half wavelengths are labeled as $\Lambda 1$ and $\Lambda 3$ along *Ox1* and *Ox3* directions, respectively. The equation of the median surface can be expressed as

$$x_2 = F(x_1, x_3) = \varepsilon f(x_1, x_3) \tag{2.84}$$

The stress-strain relationship for the midsurface can be defined by using the local coordinate system *Ox1*, *Ox2*, and *Ox3*:

$$\sigma_i = A_{ij}^{\circ} \varepsilon_j \tag{2.85a}$$

where

$$\sigma_i = \sigma_{ii} \ (i = 1,2,3) \tag{2.85b}$$

$$\varepsilon_i = \varepsilon_{ii} \ (i = 1,2,3) \tag{2.85c}$$

$$\sigma_4 = \sigma_{23} \tag{2.85d}$$

$$\sigma_5 = \sigma_{13} \tag{2.85e}$$

$$\sigma_6 = \sigma_{12} \tag{2.85f}$$

$$\varepsilon_4 = \varepsilon_{23} \tag{2.85g}$$

$$\varepsilon_5 = \varepsilon_{13} \tag{2.85h}$$

$$\varepsilon_6 = \varepsilon_{12} \tag{2.85i}$$

These relationships can also be expressed in global coordinates:

$$\sigma_i = A_{ij} \varepsilon_j \quad i, j = 1,2,3,4,5,6 \tag{2.86}$$

where the material constants in global coordinates are functions of the equation of the median surface:

$$A_{ij} = A_{ij}\left(A_{nm}^{\circ}, F(x_1, x_3)\right) \tag{2.87}$$

By satisfying the following condition

$$\varepsilon^2\left[\left(\frac{\partial f}{\partial x_1}\right)^2+\left(\frac{\partial f}{\partial x_3}\right)^2\right]<1 \quad 0\le\varepsilon<1 \tag{2.88}$$

The material constants can be expressed as

$$A_{ij}=\begin{cases} A_{ij}^{\circ}+\sum_{k=1}^{\infty}\varepsilon^{2k}A_{ijk} & \text{for combinations } ij=11,12,13,22,23,33,44,55,66 \\ \sum_{k=1}^{\infty}\varepsilon^{2k-1}A_{ijk} & \text{for combinations } ij=14,16,24,26,34,45,56 \\ \sum_{k=1}^{\infty}\varepsilon^{2k}A_{ijk} & \text{for combinations } ij=15,25,35,46 \end{cases} \tag{2.89}$$

Explicit forms of A_{ijk} are given in Ref. [33]. Moreover, by using Eq. (2.89), Eq. (2.86) can be rewritten as

$$\sigma_{ij}=\mu_{ij\alpha\beta}\frac{\partial u_\alpha}{\partial x_\beta} \quad i,j,\alpha,\beta=1,2,3 \tag{2.90}$$

where

$$\mu_{ij\alpha\beta}=\mu^0_{ij\alpha\beta}+\sum\nolimits_{k=1}^{\infty}\varepsilon^{2k-1}\mu^{(2k)}_{ij\alpha\beta}+\sum\nolimits_{k=1}^{\infty}\varepsilon^{2k}\mu^{(2k)}_{ij\alpha\beta} \tag{2.91}$$

Explicit forms of $\mu^{0}_{ij\alpha\beta}$, $\mu^{(2k-1)}_{ij\alpha\beta}$, and $\mu^{(2k)}_{ij\alpha\beta}$ are given in Ref. [32]. Finally, the equation of motion, that is,

$$\frac{\partial\sigma_{ij}}{\partial x_j}=\rho\frac{\partial^2 u_i}{\partial t^2} \tag{2.92}$$

can be written by utilizing the expressions given in Eqs. (2.90), (2.91), as

$$L_{i\alpha}u_\alpha+\sum\nolimits_{k=1}^{\infty}\varepsilon^{2k}K_{i\alpha k}u_\alpha+\sum\nolimits_{k=1}^{\infty}\varepsilon^{2k-1}R_{i\alpha k}u_\alpha=0 \tag{2.93}$$

where

$$L_{i\alpha}=\mu^{(0)}_{ij\alpha\beta}\frac{\partial^2}{\partial x_j\partial x_\beta}-\rho\delta_i^\alpha\frac{\partial^2}{\partial t^2} \tag{2.94a}$$

$$K_{i\alpha k}=\frac{\partial}{\partial x_j}\left(\mu^{(2k)}_{ij\alpha\beta}\frac{\partial}{\partial x_\beta}\right) \tag{2.94b}$$

$$R_{i\alpha k} = \frac{\partial}{\partial x_j}\left(\mu_{ij\alpha\beta}^{(2k-1)}\frac{\partial}{\partial x_\beta}\right) \tag{2.94c}$$

and δ is the Kronecker delta.

It is not possible to obtain closed-form solutions for Eq. (2.93). However, an approximate solution can be obtained by expressing physical quantities in the series of the small parameter, ε:

$$\sigma_{ij} = \sum_{q=0}^{\infty}\varepsilon^q\sigma_{ij}^{(q)} \tag{2.95a}$$

$$\varepsilon_{ij} = \sum_{q=0}^{\infty}\varepsilon^q\varepsilon_{ij}^{(q)} \tag{2.95b}$$

$$u_i = \sum_{q=0}^{\infty}\varepsilon^q u_i^{(q)} \tag{2.95c}$$

$$P_j = \sum_{q=0}^{\infty}\varepsilon^q P_j^{(q)} \tag{2.95d}$$

$$\varphi_i = \sum_{q=0}^{\infty}\varepsilon^q\varphi_i^{(q)} \tag{2.95e}$$

Hence, the equation of motion can be rewritten as (Fig. 2.11)

$$L_{i\alpha}u_\alpha^{(q)} + \sum_{k=1}^{q/2}K_{i\alpha k}u_\alpha^{(q-2k)} + \sum_{k=1}^{(q+1)/2}R_{i\alpha k}u_\alpha^{(q+1-2k)} = 0 \tag{2.96}$$

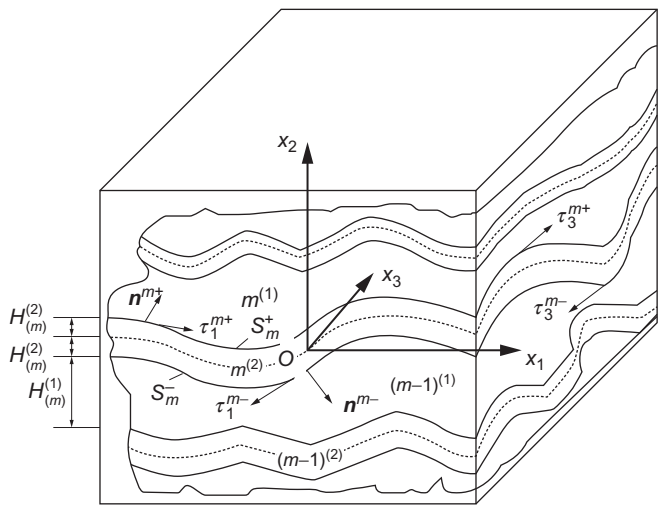

Fig. 2.11 Laminated composite [32].

The formulation can also be extended for laminated composites by imposing complete cohesion conditions between the layers:

$$\sigma_{ij}^{(1)m}|_{S_m^+} n_j^{m,+} = \sigma_{ij}^{(2)m}|_{S_m^+} n_j^{m,+}, \quad \sigma_{ij}^{(1)m_1}|_{S_m^-} n_j^{m,-} = \sigma_{ij}^{(2)m_1}|_{S_m^-} n_j^{m,-} \tag{2.97a}$$

$$u_i^{(1)m}|_{S_m^+} = u_i^{(2)m}|_{S_m^+}, \quad u_i^{(1)m_1}|_{S_m^-} = u_i^{(2)m_1}|_{S_m^-} \tag{2.97b}$$

where s_m^+ and s_m^- are upper and lower surfaces of the $m^{(2)}$ th filler layer $m_1 = m - 1$.

2.7 Strength failure theories

2.7.1 Introduction

Since a composite material is obviously heterogeneous at the constituent material level, material properties and stress-strain relations may change from point to point. However, the macromechanical stress-strain relations of a lamina can be expressed in terms of average values of stress and strain and effective properties of an equivalent homogenous material [34]. In this part, first, the constitutive equations for an orthotropic material will be introduced. Then, determination of strength and stiffness of an orthotropic lamina will be emphasized. Finally, biaxial strength criteria regarding an orthotropic lamina will be acquainted.

2.7.2 Constitutive equations for orthotropic materials

A unidirectionally reinforced lamina in the L-T plane is illustrated in Fig. 2.12. For this lamina, a state of plane stress can be defined by the settings

$$\sigma_Z = 0 \quad \tau_{TZ} = 0 \quad \tau_{ZL} = 0 \tag{2.98}$$

and

$$\sigma_L \neq 0 \quad \sigma_T \neq 0 \quad \tau_{LT} \neq 0 \tag{2.99}$$

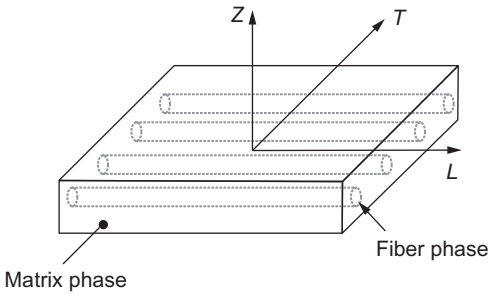

Fig. 2.12 Principal material axes for an orthotropic lamina.

The state of plane stress is an idealization for practical usage of a lamina having fibers in its plane. It is considered that a single lamina can withstand against only in-plane loadings since its capability of load carrying in-plane is natural. Some examples such as automobile panels, thin-pressure vessels, fuselages, and wings of aircraft may be given for the in-plane loaded structural elements [35].

For an orthotropic lamina imposed to the plane stress state, the following strains emerge in the out-of-plane

$$\varepsilon_Z = S_{13}\sigma_L + S_{23}\sigma_T \quad \gamma_{TZ} = 0 \quad \gamma_{ZL} = 0 \tag{2.100}$$

where

$$S_{13} = -\frac{\nu_{LZ}}{E_L} = -\frac{\nu_{ZL}}{E_Z} \quad S_{23} = -\frac{\nu_{TZ}}{E_T} = -\frac{\nu_{ZT}}{E_Z} \tag{2.101}$$

The strain-stress relations in the L-T plane is written in the matrix form as

$$\begin{Bmatrix} \varepsilon_L \\ \varepsilon_T \\ \gamma_{LT} \end{Bmatrix} = \begin{bmatrix} S_{11} & S_{12} & 0 \\ S_{12} & S_{22} & 0 \\ 0 & 0 & S_{66} \end{bmatrix} \begin{Bmatrix} \sigma_L \\ \sigma_T \\ \tau_{LT} \end{Bmatrix} \text{ or } \begin{Bmatrix} \varepsilon_L \\ \varepsilon_T \\ \gamma_{LT} \end{Bmatrix} = [S] \begin{Bmatrix} \sigma_L \\ \sigma_T \\ \tau_{LT} \end{Bmatrix} \tag{2.102}$$

where square matrix is the compliance matrix $[S_{ij}]$, members of which are given in terms of the engineering constants as

$$S_{11} = \frac{1}{E_L} \quad S_{22} = \frac{1}{E_T} \quad S_{12} = -\frac{\nu_{LT}}{E_L} = -\frac{\nu_{TL}}{E_T} \quad S_{66} = \frac{1}{G_{LT}} \tag{2.103}$$

When Eq. (2.102) is inverted, the stress-strain relations are written as

$$\begin{Bmatrix} \sigma_L \\ \sigma_T \\ \tau_{LT} \end{Bmatrix} = \begin{bmatrix} Q_{11} & Q_{12} & 0 \\ Q_{12} & Q_{22} & 0 \\ 0 & 0 & Q_{66} \end{bmatrix} \begin{Bmatrix} \varepsilon_L \\ \varepsilon_T \\ \gamma_{LT} \end{Bmatrix} \text{ or } \begin{Bmatrix} \sigma_L \\ \sigma_T \\ \tau_{LT} \end{Bmatrix} = [Q] \begin{Bmatrix} \varepsilon_L \\ \varepsilon_T \\ \gamma_{LT} \end{Bmatrix} \tag{2.104}$$

where the $[Q]$ is the so-called reduced stiffness matrix, members of which are written in terms of the engineering constants (see Eq. 2.10).

From the Q_{12} given by Eq. (2.10), the following reciprocal relation reveals

$$\nu_{TL}E_L = \nu_{LT}E_T \quad \text{or} \quad \frac{\nu_{LT}}{E_L} = \frac{\nu_{TL}}{E_T} \tag{2.105}$$

2.7.2.1 Stress-strain relations for a lamina of arbitrary orientation

Because the laminates have low stiffness and strength properties in the transverse direction, they are not often formed only as unidirectional laminae. For this purpose,

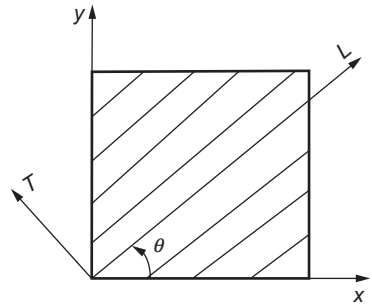

Fig. 2.13 Positive rotation of principal material axes from *x*-*y* axes.

some laminae in the laminates may be placed at different angles. It is thus necessary to develop the stress-strain or the strain-stress relations for an angle lamina. The coordinate systems used for an angle lamina are given in Fig. 2.13. The axes *L*-*T* are called the principal material or local axes, in which the direction *L* is parallel to the fibers and the direction *T* is perpendicular (transverse) to the fibers. The axes *x*-*y* are called the global axes or the off axes. The angle between the two axes is denoted by an angle θ. A relation is, now, needed between the stresses and strains and those in the structure axes. Then, stress-strain relations should be transformed from one coordinate system to another.

At this point, the global and local stresses in any angle lamina are related to each other through the reinforcement angle, θ:

$$\begin{Bmatrix} \sigma_L \\ \sigma_T \\ \tau_{LT} \end{Bmatrix} = [T] \begin{Bmatrix} \sigma_x \\ \sigma_y \\ \tau_{xy} \end{Bmatrix} \quad \text{and} \quad \begin{Bmatrix} \sigma_x \\ \sigma_y \\ \tau_{xy} \end{Bmatrix} = [T]^{-1} \begin{Bmatrix} \sigma_L \\ \sigma_T \\ \tau_{LT} \end{Bmatrix} \tag{2.106}$$

where $[T]$ and $[T]^{-1}$ are the transformation matrix and its inverse, which are defined taking as $s = sin\ \theta$ and $c = cos\ \theta$:

$$[T] = \begin{bmatrix} c^2 & s^2 & -2cs \\ s^2 & s^2 & 2cs \\ cs & -cs & c^2 - s^2 \end{bmatrix} \quad \text{and} \quad [T]^{-1} = \begin{bmatrix} c^2 & s^2 & 2cs \\ s^2 & s^2 & -2cs \\ -cs & cs & c^2 - s^2 \end{bmatrix} \tag{2.107}$$

Similarly, the strain-transformation equations are as

$$\begin{Bmatrix} \varepsilon_L \\ \varepsilon_T \\ \frac{1}{2}\gamma_{LT} \end{Bmatrix} = [T] \begin{Bmatrix} \varepsilon_x \\ \varepsilon_y \\ \frac{1}{2}\gamma_{xy} \end{Bmatrix} \quad \text{and} \quad \begin{Bmatrix} \varepsilon_x \\ \varepsilon_y \\ \frac{1}{2}\gamma_{xy} \end{Bmatrix} = [T]^{-1} \begin{Bmatrix} \varepsilon_L \\ \varepsilon_T \\ \frac{1}{2}\gamma_{LT} \end{Bmatrix} \tag{2.108}$$

However, with a matrix $[R]$ introduced by Reuter,

$$[R] = \begin{bmatrix} 1 & 0 & 0 \\ 0 & 1 & 0 \\ 0 & 0 & 2 \end{bmatrix} \tag{2.109}$$

the strain-transformation equations can be rewritten as

$$\begin{Bmatrix} \varepsilon_L \\ \varepsilon_T \\ \gamma_{LT} \end{Bmatrix} = [R] \begin{Bmatrix} \varepsilon_L \\ \varepsilon_T \\ \frac{1}{2}\gamma_{LT} \end{Bmatrix} \quad \text{and} \quad \begin{Bmatrix} \varepsilon_x \\ \varepsilon_y \\ \gamma_{xy} \end{Bmatrix} = [R] \begin{Bmatrix} \varepsilon_x \\ \varepsilon_y \\ \frac{1}{2}\gamma_{xy} \end{Bmatrix} \tag{2.110}$$

When Eqs. (2.102, 2.104, 2.106–2.110) obtained above are combined according to the rules of matrix, the stress-strain relations in x-y plane are found as [3,35]

$$\begin{Bmatrix} \sigma_x \\ \sigma_y \\ \tau_{xy} \end{Bmatrix} = [T]^{-1} \begin{Bmatrix} \sigma_L \\ \sigma_T \\ \tau_{LT} \end{Bmatrix} = [T]^{-1}[Q][R][T][R]^{-1} \begin{Bmatrix} \varepsilon_x \\ \varepsilon_y \\ \gamma_{xy} \end{Bmatrix} \tag{2.111}$$

in which $[R][T][R]^{-1}$ is shortly $[T]^{-T}$ where the superscript T denotes the matrix transpose. With the use of abbreviation in the form of $\left[\bar{Q}\right] = [T]^{-1}[Q][T]^{-T}$, the stress-strain relations in x-y coordinates becomes

$$\begin{Bmatrix} \sigma_x \\ \sigma_y \\ \tau_{xy} \end{Bmatrix} = \left[\bar{Q}\right] \begin{Bmatrix} \varepsilon_x \\ \varepsilon_y \\ \gamma_{xy} \end{Bmatrix} = \begin{bmatrix} \bar{Q}_{11} & \bar{Q}_{12} & \bar{Q}_{16} \\ \bar{Q}_{12} & \bar{Q}_{22} & \bar{Q}_{26} \\ \bar{Q}_{16} & \bar{Q}_{26} & \bar{Q}_{66} \end{bmatrix} \begin{Bmatrix} \varepsilon_x \\ \varepsilon_y \\ \gamma_{xy} \end{Bmatrix} \tag{2.112}$$

in which $\left[\bar{Q}\right]$ denotes the transformed reduced stiffness matrix (see Eq. 2.9).

Similarly, the strain-stress relations in x-y coordinates can be written as

$$\begin{Bmatrix} \varepsilon_x \\ \varepsilon_y \\ \gamma_{xy} \end{Bmatrix} = [\bar{S}] \begin{Bmatrix} \sigma_x \\ \sigma_y \\ \tau_{xy} \end{Bmatrix} = \begin{bmatrix} \bar{S}_{11} & \bar{S}_{12} & \bar{S}_{16} \\ \bar{S}_{12} & \bar{S}_{22} & \bar{S}_{26} \\ \bar{S}_{16} & \bar{S}_{26} & \bar{S}_{66} \end{bmatrix} \begin{Bmatrix} \sigma_x \\ \sigma_y \\ \tau_{xy} \end{Bmatrix} \tag{2.113}$$

in which the $[\bar{S}]$ denotes the transformed reduced compliance matrix, elements of which are written similar to the $\left[\bar{Q}\right]$

$$\begin{aligned}
\bar{S}_{11} &= S_{11}c^4 + (2S_{12} + S_{66})s^2c^2 + S_{22}s^4 \\
\bar{S}_{22} &= S_{11}s^4 + (2S_{12} + S_{66})s^2c^2 + S_{22}c^4 \\
\bar{S}_{12} &= (S_{11} + S_{22} - S_{66})s^2c^2 + S_{12}\left(s^4 + c^4\right) \\
\bar{S}_{16} &= 2(S_{11} - S_{12} - 0.5S_{66})sc^3 - 2(S_{22} - S_{12} - 0.5S_{66})s^3c \\
\bar{S}_{26} &= 2(S_{11} - S_{12} - 0.5S_{66})s^3c + 2(S_{22} - S_{12} - 0.5S_{66})sc^3 \\
\bar{S}_{66} &= 4(S_{11} + S_{22} - 2S_{12} - 0.5S_{66})s^2c^2 + S_{66}\left(s^4 + c^4\right)
\end{aligned} \tag{2.114}$$

2.7.3 Determination of strength and stiffness of an orthotropic lamina

Both strength and stiffness characteristics of an orthotropic lamina are reasonably necessary for the design of laminates. The axes of principal stress do not coincide with the axes of principal strain due to orthotropy. In a given lamina, the strength in one direction can be higher than another; the highest stress might not be the stress governing the design. Therefore, a rational comparison of the actual stress field with the allowable stress field can be required, irrespective of any principal values. The first step in such a procedure is the establishments of the allowable stresses or strengths in the principal material directions, which is the basic of the study of strength for an orthotropic lamina [35].

The three basic strengths in a lamina under in-plane loading can be mentioned, which are shown in Fig. 2.14 when the tensile strength is equal to the compressive strength in it:

X is the axial (longitudinal) strength (in the 1-direction)
Y is thetransverse strength (in the 2-direction)
S is the shear strength (in the 1–2 plane)

If a lamina has different mechanical properties in tension and compression, five strengths are needed as

X_t is the axial (longitudinal) strength in tension
X_c is the axial (longitudinal) strength in compression
Y_t is the transverse strength in tension
Y_c is the transverse strength in compression
S is the shear strength

2.7.3.1 Determination of stiffness and strength for a lamina

The properties (stiffness and strength) in the principal material axis can be determined with some experiments. If the experiments are performed properly, the strength and stiffness values of the material may be adequately revealed. The stiffness characteristics of a lamina are listed as follows:

E_L is the Young's modulus in the longitudinal (fiber) direction
E_T is the Young's modulus in the transverse direction
G_{LT} is the Shearing modulus
ν_{LT} is the Major Poisson's ratio
ν_{TL} is the Minor Poisson's ratio

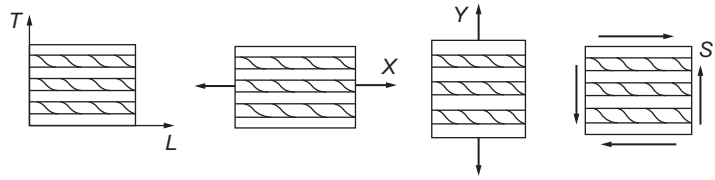

Fig. 2.14 Basic strengths for orthotropic lamina.

where only three of E_L, E_T, ν_{LT}, and ν_{TL} are independent. E_L and ν_{LT} may be measured by a tension-test fixture using a sample in the fiber direction. While the normal strain-strain (ε_L-σ_L) values in the fiber direction are sufficient for E_L, the transverse (ε_T) strain in addition to ε_L is necessary for determination of Poisson's ratio ν_{LT}. Similarly, E_T and ν_{TL} may be measured by a tension-test fixture using a sample in the transverse direction. While the normal strain-strain (ε_T-σ_T) values in the transverse direction are sufficient for E_T, the transverse (ε_L) strain in addition to ε_T is needed for Poisson's ratio ν_{TL}. Upon determination of these for the elastic properties, the satisfaction in terms of correctness of the conducted experiments may be done with Eq. (2.105) as follows:

$$\frac{\nu_{LT}}{E_L} = \frac{\nu_{TL}}{E_T} \tag{2.115}$$

For the determination of the remaining property G_{12}, there are several experimental techniques such as 45° off-axis test, torsion-tube test, sandwich crossbeam test, rail shear test, and Iosipescu test.Also, the strength characteristics for a lamina are listed as follows:

X (X_t or X_c) is the Longitudinal (tensile or compressive) strength (L-direction)
Y (Y_t or Y_c) is the Transverse (tensile or compressive) strength (T-direction)
S is the Shear strength (L-T plane)

where tensile or compressive strengths are of different values for some materials. The strengths X (X_t or X_c) and Y (Y_t or Y_c) can be determined by a tensile test machine. The shear strength S may be obtained by means of experiments such as torsion-tube test, rail shear test, and Iosipescu test [34,35].

2.7.4 Biaxial strength criteria for an orthotropic lamina

Although the strength of a material is determined by uniaxial tests, in fact, the structural elements may be exposed to biaxial or triaxial state of stress. Therefore, uniaxial strength values obtained for principal axis are classed with those of multiaxial loading conditions for the design of elements of machine and structure.

The strengths of principal material directions are X_t, X_c, Y_t, and Y_c, which are tensile and compressive strength in the fiber direction and transverse direction, respectively, and S is shearing strength. However, since tensile and compressive strengths of some materials are same, they are described as X in the fiber direction and Y in transverse direction.

Some criteria such as the maximum normal, the maximum shearing (Tresca), and the maximum distortional energy (von Mises) are fairly well for the conventional engineering materials, which are accepted as isotropic. Unfortunately, these theories are not adequate for composite materials. For this reason, the following biaxial strength criteria that are commonly exploited for the design of composites will be examined: (a) Tsai-Hill failure criterion, (b) Hoffman failure criterion, and (c) Tsai-Wu tensor failure criterion. In the implementations of these criteria, composite material is regarded as orthotropic and homogeneous, and the stress components

calculated from the loadings at the different angles are needed to be transformed into the biaxial stress components in the principal material axis.

2.7.4.1 Tsai-Hill failure criterion

Tsai-Hill failure criterion, which is related to the amount of distortion energy rather than dilatation for any isotropic body, is an adapted version of von Mises' yield criterion to orthotropic composite plates. It is, however, known that distortion is not independent from dilatation in orthotropic materials. Although detailed information given in the bibliography [35], Tsai-Hill failure criterion for an orthotropic plate can be expressed in the form:

$$\frac{\sigma_L^2}{X^2} - \frac{\sigma_L \sigma_T}{X^2} + \frac{\sigma_T^2}{Y^2} + \frac{\tau_{LT}^2}{S^2} = 1 \tag{2.116}$$

where σ_L, σ_T, and τ_{LT} are the transformed stresses into the principle axis and X, Y, and S are failure principle strengths for a single orthotropic lamina. Here, X_t or X_c and Y_t or Y_c should be employed depending on the signs of σ_L and σ_T. According to this theory, when Eq. (2.116) is greater than or equal to 1, the lamina is accepted to be damaged.

It is reported that the agreement is quite good between the Tsai-Hill failure criterion and experiment from the results obtained, for some materials, for example, the E-glass-epoxy at various orientations in biaxial stress states [35]. Hence, the Tsai-Hill failure criterion is applicable to failure prediction for composite materials. However, the applicability of a failure criterion depends on whether the material is brittle or ductile. Therefore, it would be advisable to browse other some criteria.

2.7.4.2 Hoffman failure criterion

Some materials, when subjected to tensile and compressive loadings, exhibit different behaviors. On this occasion, Hoffman had developed an equation for especially brittle materials inspired by the Tsai-Hill failure criterion. Hoffman failure criterion can be expressed in the following form:

$$-\frac{\sigma_L^2}{X_c X_t} + \frac{\sigma_L \sigma_T}{X_c X_t} - \frac{\sigma_T^2}{Y_c Y_t} + \frac{X_c + X_t}{X_c X_t}\sigma_1 + \frac{Y_L + Y_T}{Y_c Y_t}\sigma_2 + \frac{\tau_{LT}^2}{S^2} = 1 \tag{2.117}$$

The Hoffman failure criterion comes to the same point with the Tsai-Hill criterion for equal strength values in tension and compression. It is noted that the Hoffman failure criterion is in good agreement with some materials such as glass-epoxy, graphite-epoxy, and boron-epoxy [35].

2.7.4.3 Tsai-Wu tensor failure criterion

This failure theory is based on the total strain energy failure theory of Beltrami, which is widely used for composite materials with different strengths in tension and compression [3,36]. Even if the proceeding biaxial failure criteria give very good results

for some materials, they are inadequate in their representation of experimental data for some other materials. For this purpose, Tsai and Wu had improved the correlation between a criterion and experiment, which increased the number of terms in the prediction equation. In order to symbolize the interaction between stresses in two directions a new strength should be defined.

Tsai and Wu had postulated a new formula for the Tsai-Wu tensor failure criterion that considerably resembles the Tsai-Hill failure criterion as follows:

$$\frac{\sigma_L^2}{X^2} - 2F_{12}\sigma_L\sigma_T + \frac{\sigma_T^2}{Y^2} + \frac{\tau_{LT}^2}{S^2} = 1 \tag{2.118}$$

where F_{12}, a coefficient of the product of σ_1 and σ_2, is not $-X^{-2}$ and thus it differs from the Tsai-Hill failure criterion. F_{12} can be determined with only a biaxial tension test described by $\sigma_1 = \sigma_2 = \sigma$, and all other stresses are zero. For calculating the value of F_{12}, an empirical expression is suggested as [3]

$$F_{12} = -\frac{1}{2}\sqrt{\frac{1}{X_t X_c Y_t Y_c}} \tag{2.119}$$

Since the Tsai-Wu tensor failure criterion discriminates between the compressive and tensile strengths of a lamina, this failure theory has more general use than the Tsai-Hill failure theory.

2.8 Dynamic behavior of composites

This section presents dynamic behavior of composites by discussing longitudinal vibration of bars, transverse vibration of beams and laminated plates, and damping analysis of composites.

2.8.1 Longitudinal vibrations in composite bars

Linear longitudinal vibrations in a homogeneous isotropic bar (Fig. 2.15) are governed by the equation:

$$\frac{\partial}{\partial x}\left(AE\frac{\partial u}{\partial x}\right) = \rho A\frac{\partial^2 u}{\partial t^2} \tag{2.120}$$

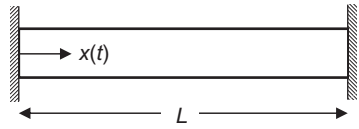

Fig. 2.15 Linear fixed-fixed bar of length L and cross-sectional area A.

where x is the distance from the left end of the bar, t is time, u is the longitudinal displacement of cross section $A(x)$ at a distance x from end of the bar and time t, ρ is mass density of the bar, and $E(x)$ is the modulus of elasticity of the bar.

As for a heterogeneous linear elastic composite bar, the density ρ and the elasticity modulus E in Eq. (2.120) can be replaced with the effective properties of an equivalent homogeneous material. The effective modulus E will specifically depend on the orientation of fibers relative to the axis of the bar, namely, $E = E_1$ and $E = E_2$ for longitudinal and transverse directions, respectively.

If the cross-sectional area and the elasticity modulus are constants, Eq. (2.120) will reduce to

$$c^2 \frac{\partial^2 u}{\partial x^2} = \frac{\partial^2 u}{\partial t^2} \tag{2.121}$$

where c is the wave speed and given as $c = \sqrt{E/\rho}$.

Separation of variables can be used to solve Eq. (2.121) by assuming a solution of the form:

$$u(x,t) = \chi(x)T(t) \tag{2.122}$$

where $\chi(x)$ is a function of x alone, but not on t, and $T(t)$ is a function of t alone, but not on x. When this assumed solution is substituted into Eq. (2.121), then variables are separated:

$$c^2 \frac{1}{\chi}\frac{d^2\chi}{dx^2} = \frac{1}{T}\frac{d^2T}{dt^2} \tag{2.123}$$

is obtained. The left-hand side of Eq. (2.123) is a function of x alone, but not on t, and the right-hand side of it is a function of t alone, but not on x, which can be possible only if both are equal to a constant, and let this constant be $-\omega^2$. Then, Eq.(2.123) can be written as two ordinary differential equations as follows:

$$\frac{d^2T}{dt^2} + \omega^2 T = 0 \tag{2.124a}$$

$$\frac{d^2\chi}{dx^2} + \left(\frac{\omega}{c}\right)^2 \chi = 0 \tag{2.124b}$$

Solutions to these equations are given in the form of

$$T(t) = c_1 \sin \omega t + c_2 \cos \omega t \tag{2.125a}$$

$$\chi(x) = c_3 \sin \frac{\omega}{c}x + c_4 \cos \frac{\omega}{c}x \tag{2.125b}$$

where constants c_1 and c_2 can be determined from initial conditions and constants c_3 and c_4 can be determined from boundary conditions. When boundary conditions of

$u(0,t)=0$ and $u(L,t)=0$ for a fixed-fixed bar is substituted into Eq. (2.125b), $c_4=0$ and

$$sin\frac{\omega}{c}L=0 \tag{2.126}$$

are found. Similarly, boundary conditions for other types of end supports can easily be found in any vibration books.

Eq. (2.126) is an eigenvalue equation, and hence, it has an infinite number of solutions as follows:

$$\frac{\omega_n L}{c}=n\pi \quad n=1,2,\ldots \tag{2.127}$$

where n is the mode number and ω_n natural frequencies in radians per seconds. Therefore, displacements for the nth mode of vibration is given as

$$u_n(x,t)=(A\,sin\,\omega_n t+B\,cos\,\omega_n t)sin\frac{n\pi x}{L} \tag{2.128}$$

where $A=c_1c_3$ and $B=c_2c_3$. The eigenfunction providing the mode shape for the nth mode is given by

$$\chi_n(x)=sin\frac{n\pi x}{L} \tag{2.129}$$

Finally, the general solution is obtained by summing up all modal responses as follows:

$$u(x,t)=\sum\nolimits_{n=1}^{\infty}(A\,sin\,\omega_n t+B\,cos\,\omega_n t)sin\frac{n\pi x}{L} \tag{2.130}$$

Mode shapes and natural frequencies for the first three modes are depicted in Fig. 2.16 for a fixed-fixed bar of length L, cross-sectional area A, and modulus of elasticity E.

One of the basic approaches for determining mechanical properties of composite materials is vibration experiments. Specifically, if the natural frequency of the nth mode is measured in an experiment, one can easily determine the effective modulus of the composite material.

2.8.2 Transverse vibration of composite beams

Linear transverse vibration of a homogeneous, isotropic, elastic beam (Fig. 2.17) can be governed by the Bernoulli-Euler-type equation without taking into consideration shear and rotary inertia effects during the formulation, which is given as

$$-\frac{\partial^2}{\partial x^2}\left(EI\frac{\partial^2 w}{\partial x^2}\right)=\rho A\frac{\partial^2 w}{\partial t^2} \tag{2.131}$$

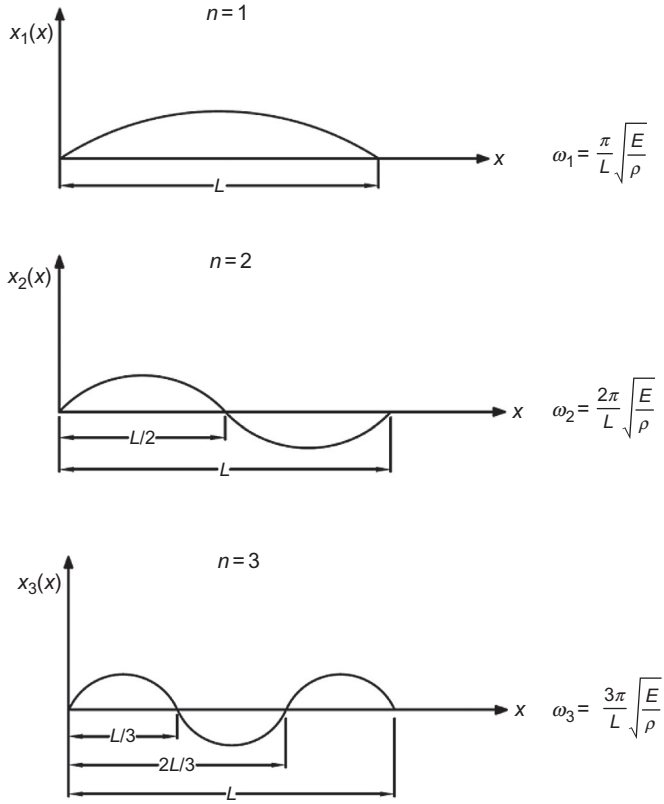

Fig. 2.16 Mode shapes and natural frequencies of a fixed-fixed bar for the first three modes of longitudinal vibration.

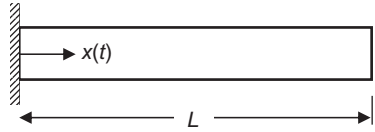

Fig. 2.17 Cantilever beam in transverse vibration.

where I is the moment of inertia of the cross section about the neutral axis of the beam while $w = w(x, t)$ is the transverse displacement of the same axis of the beam. Other constants, that is, x, t, ρ, A, and E, are as defined in previous section. If EI is constant across the beam, then the governing equation reduces to

$$EI\frac{\partial^4 w}{\partial x^4} + \rho A\frac{\partial^2 w}{\partial t^2} = 0 \tag{2.132}$$

This equation can be solved for orthotropic composite beams using separation variables again by assuming that modulus E can be replaced by the effective modulus E_f.

Assuming a solution in the form of

$$w(x,t) = W(x)e^{i\omega_n t} \tag{2.133}$$

yields an ordinary differential equation of the form:

$$\frac{d^4W(x)}{dx^4} - k^4W(x) = 0 \tag{2.134}$$

where ω is the frequency, $W(x)$ is the mode shape function, and the constant k is given as

$$k = \left(\frac{\omega^2\rho A}{EI}\right)^{1/4} \tag{2.135}$$

The solution for Eq. (2.134) is given as follows:

$$W(x) = C_1 sin\, kx + C_2 cos\, kx + C_3 sinh\, kx + C_4 cosh\, kx \tag{2.136}$$

where the constants C_1, C_2, C_3, and C_4 can be determined by applying boundary conditions. A detailed explanation of boundary conditions and their applications is beyond the scope of this book and can be found in a vibration book covering continuous vibrations.

The eigenvalue equation resulted by the application of boundary conditions is solved to determine natural frequencies and mode shapes of the vibrating system. As an illustration, for a cantilever beam, the natural frequency equation is given as

$$\omega_n = k_n^2\sqrt{\frac{EI}{\rho A}} \quad n = 1, 2, 3, \ldots \tag{2.137}$$

where n is the mode number, and for the first three modes, they are computed as $k_nL = 1.875, 4.694, 7855$. First three mode shapes for a cantilever beam are shown on Fig. 2.18.

2.8.3 Transverse vibration of orthotropic plates

In this section, a general equation of motion for a laminated composite plate in transverse vibration is simply presented. Summation of forces acting on an infinitesimal element can be written according to Newton's second law as

$$\frac{\partial N_x}{\partial x} + \frac{\partial N_{xy}}{\partial y} = \rho_0\frac{\partial^2 u^0}{\partial t^2} \tag{2.138}$$

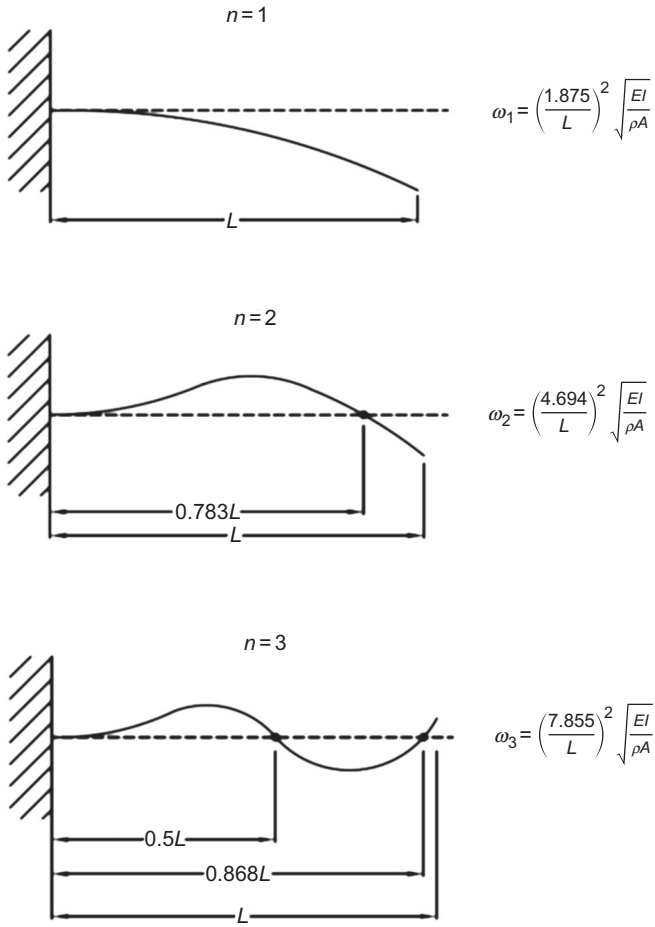

Fig. 2.18 Mode shapes and natural frequencies for the first three modes of transverse vibration of the cantilever beam.

$$\frac{\partial N_y}{\partial y} + \frac{\partial N_{xy}}{\partial x} = \rho_0 \frac{\partial^2 v^0}{\partial t^2} \tag{2.139}$$

$$\frac{\partial Q_x}{\partial x} + \frac{\partial Q_y}{\partial y} + q(x, y) = \rho_0 \frac{\partial^2 w}{\partial t^2} \tag{2.140}$$

where N's and Q's are respective in-plane stress resultants and ρ_0 is the mass per unit area of the laminate. The displacements u, v, and w are in the directions of x, y, and z, while the superscript zero shows middle-surface displacements in respective directions. $q(x, y)$ stands for the transverse distributed force.

On the other hand, by neglecting rotary inertia, moments can be summed about x and y axis and then simplified to get

$$\frac{\partial M_y}{\partial y}+\frac{\partial M_{xy}}{\partial x}=Q_y \tag{2.141}$$

$$\frac{\partial M_x}{\partial x}+\frac{\partial M_{xy}}{\partial y}=Q_x \tag{2.142}$$

respectively. Eqs. (2.141), (2.142) can be substituted in Eq. (2.140) to yield

$$\frac{\partial^2 M_x}{\partial x^2}+2\frac{\partial^2 M_{xy}}{\partial x\partial y}+\frac{\partial^2 M_y}{\partial y^2}+q(x,y)=\rho_0\frac{\partial^2 w}{\partial t^2} \tag{2.143}$$

Eqs. (2.138)–(2.140), (2.143) are the equations of motion of the plate in stress and moment resultants. These equations of motion can be rewritten in terms of displacements by substituting laminate force-deformation, strain-displacement, and curvature-displacement relations into above equations and then solved for the desired boundary conditions.

As an example, results for the free transverse vibration of a rectangular orthotropic plate of size $a\times b$ are given here without proof for simply supported case. Based on the discussion of Ashton and Whitney [37], one may obtain the equation of motion of an orthotropic plate as follows:

$$D_{11}\frac{\partial^4 w}{\partial x^4}+2(D_{12}+2D_{66})\frac{\partial^4 w}{\partial x^2\partial y^2}+D_{22}\frac{\partial^4 w}{\partial y^4}+\rho_0\frac{\partial^2 w}{\partial t^2}=0 \tag{2.144}$$

where $w=w(x,y,t)$ is the displacement in z direction and D's are constants arising from the integration of some stiffness terms. By using separation of variables and applying appropriate boundary continuous, one may obtain the frequency equation as

$$\omega_{mm}^2=\frac{\pi^4}{\rho_0 a^4}\left[D_{11}m^4+2(D_{12}+2D_{66})(mnR)^2+D_{22}(nR)^4\right] \tag{2.145}$$

and the mode shape function as

$$W(x,y)=A_{mn}sin\frac{m\pi x}{a}sin\frac{n\pi y}{b} \tag{2.146}$$

where m and n are mode indexes, a and b are plate dimensions in x and y directions, respectively, and $R = a/b$ is the plate aspect ratio.

Numerical results for frequencies and mode shapes of two square plates are included here as presented by Ashton and Whitney [37]. One of the plates is orthotropic with ratios $D_{11}/D_{22}=10$ and $(D_{12}+2D_{66})/D_{22}=1$, and the other one is isotropic with ratios $D_{11}/D_{22}=1$ and $(D_{12}+2D_{66})/D_{22}=1$. Table 2.1 presents

Table 2.1 First four natural frequencies for a simply supported orthotropic and isotropic plates [37]

	Orthotropic $\omega = k\pi^2/b^2\sqrt{D_{22}/\rho_0}$			Isotropic $\omega = k\pi^2/b^2\sqrt{D/\rho_0}$		
Mode	***m***	***n***	***k***	***m***	***n***	***k***
1st	1	1	3.62	1	1	2.0
2nd	1	2	5.68	1	2	5.0
3rd	1	3	10.45	2	1	5.0
4th	2	1	13	2	2	8.0

the lowest four natural frequencies for the two plates, while Fig. 2.19 compares the corresponding mode shapes for the plates. Nodal lines are denoted by dotted lines on the figure. It is noted that sequence of mode numbers for increasing frequency differs for orthotropic and isotropic plates.

2.8.4 Analysis of damping in composites

The aim of this section is to cover linear viscoelastic damping analysis of composites. Damping is defined as the dissipation of mechanical energy during dynamic deformation of structures. In metallic structures, much of the damping is accepted to be arising from structural joints rather than damping within the metal itself. Conversely, polymer

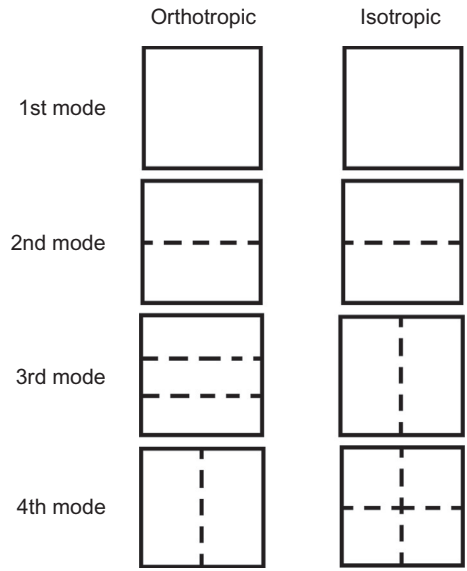

Fig. 2.19 First four mode shapes for a simply supported orthotropic and isotropic plates [37].

composites present a high damping and lightweight properties, which provides flexibility for designers pursuing a trade-off between damping and stiffness.

Damping is one of the most important aspects of structural materials under dynamic loads. Although the viscoelastic behavior of composite materials seems to be the main mechanism for damping, thermoelastic damping, coulomb friction, and cracks or delaminations are other sources of energy dissipations. Thermoelastic damping generally arises in metallic composites rather than polymer-based composites. Damping due to cracks or delaminations can be experimentally measured using some nondestructive testing methods but cannot be utilized as a criterion in the design of structures.

Some analytic damping prediction tools have been developed in the literature at either micromechanical or macromechanical level. For instance, thermoelastic and dislocation damping models are established to predict damping without the need of material-damping properties. For the viscoelastic type of damping, usually one of two approaches is tackled. The first approach comprises the utilization of elastic viscoelastic correspondence principle together with elasticity theory. The second one is related to the strain energy formulation in which the relation of total damping is established with the damping in each element.

In conclusion, since damping is an important issue in the design of dynamically loaded composite structures, its prediction has a growing interest among designers. Some analytic prediction methods have been developed in the literature and shortly pointed out here.

References

[1] Mallick PK. Fiber-reinforced composites: materials, manufacturing and design. New York, NY: CRC Press, Taylor and Francis Group; 2008.
[2] Aydin L, Artem HS. Comparison of stochastic search optimization algorithms for the laminated composites under mechanical and hygrothermal loadings. J Reinf Plast Compos 2011;30(14):1197–212.
[3] Kaw AK. Mechanics of composite materials. New York, NY: CRC Press, Taylor and Francis Group; 2006.
[4] Berthelot JM. Composite materials: mechanical behavior and structural analysis. Berlin: Springer Verlag; 1999.
[5] Daniel IM, Ishai O. Engineering mechanics of composite materials. New York: Oxford University Press; 1994.
[6] Aydin L. Design of dimensionally-stable laminated composites subjected to hygro-thermo-mechanical loading by stochastic optimization methods [Ph.D. thesis]. İzmir: İzmir Institute of Technology; 2011.
[7] Taya M, Arsenault RJ. Metal matrix composites : thermomechanical behavior. Oxford: Pergamon Press; 1989.
[8] Gültürk E. The effects of diatom frustule filling on the quasi-static and high strain rate mechanical behavior of polymer matrices [Ph.D. thesis]. İzmir: Izmir Institute of Technology; 2010.
[9] Cox HF. The elasticity and strength of paper and other fibrous materials. Br J Appl Phys 1952;3:29–72.

[10] Nairn JA. On the use of shear-lag methods for analysis of stress transferunidirectional composites. Mech Mater 1997;26(2):63–80.
[11] Garg SK, Svalbonas V, Gurtman GA. Analysis of structural composite materials. New York, NY: Marcel Dekker; 1973.
[12] Agarwal BD, Broutman LJ. Analysis and performance of fiber composites. New York, NY: J. Wiley & Sons; 1980.
[13] Chamis CC, Sendecyj GP. Critique on theories predicting thermoelastic properties of fibrous composites. J Compos Mater 1968;2:332.
[14] Lingois P, Berglund L. Modeling elastic properties and volume change in dental composites. J Mater Sci 2002;37:4573–9.
[15] Mcgee SH, Mccullough RL. Models for the permeability of filled polymer systems. Polym Compos 1981;2:149.
[16] Hermans JJ. The elastic properties of fiber reinforced materials when the fibers are aligned. Proc K Ned Akad Wet Ser B 1967;65:1–9.
[17] Hill RJ. Theory of mechanical properties of fibre-strengthened materials. I. Elastic behaviour. J Mech Phys Solids 1964;12:199.
[18] Whitney JM, McCullough RL. Delaware composites design encyclopedia: micromechanical materials modeling, vol 2. Pennsylvania: Technomic Publishing; 1990.
[19] Halpin JC, Kardos JL. The Halpin-Tsai equations: a review. Polym Eng Sci 1976;16:344–52.
[20] Nielsen LE. Generalized equation for the elastic moduli of composite materials. J Appl Phys 1970;41:4626–7.
[21] Lewis TB, Nielsen LE. Dynamic mechanical properties of particulate-filled composites. J Appl Polym Sci 1970;14:1449–71.
[22] Chantler PM, Hu X, Boyd NM. An extension of a phenomenological model for dental composites. Dent Mater 1999;15:144–9.
[23] Braem M, Van Doren VE, Lambreehts P, Vanherle G. Determination of young's modulus of dental composites. A phenomenological model. J Mater Sci 1987;22:2037–42.
[24] Guth E, Gold O. New foundation of general relativity. Phys Rev 1938;53:322.
[25] Guth E. Theory of filler reinforcement. J Appl Phys 1945;16:20.
[26] Wu YP, Jia QX, Yu DS, Zhang LQ. Modeling young's modulus of rubber-clay nanocomposites using composite theories. Polym Test 2004;23:903–9.
[27] Mooney M. The viscosity of a concentrated suspension of spherical particles. J Colloid Sci 1951;6:162–70.
[28] Brodnyan JG. The concentration dependence of the Newtonian viscosity of prolate ellipsoids. Trans Soc Rheol 1959;3:61.
[29] Akkerman R. Laminate mechanics for balanced woven fabrics. Compos Part B 2006;37:108–16.
[30] Chou TW, Ko FK. Textile structural composites. New York, NY: Elsevier Science Publishing Company; 1989.
[31] Lei Z, Li X, Qin F, Qiu W. Interfacial micromechanics in fibrous composites: design, evaluation, and models. Sci World J 2014;2014:1–9. Article ID 282436, http://dx.doi.org/10.1155/2014/282436.
[32] Akbarov SD, Guz AN. Mechanics of curved composites and some related problems for structural members. Mech Adv Mater Struct 2004;11(6):445–515.
[33] Akbarov SD, Guz AN. Mechanics of curved composites. Dordrecht/Boston, MA/London: Kluwer Academic; 2000.

[34] Gibson RF. Principles of composite material mechanics. New York, NY: McGraw Hil; 1994.
[35] Jones RM. Mechanics of composite materials. Philadelphia: Taylor and Francis; 1999.
[36] Tsai SW, Wu EM. A general theory of strength for anisotropic materials. J Compos Mater 1971;5:58–80.
[37] Ashton JE, Whitney JM. Theory of laminated plates. Lancaster, PA: Technomic Publishing Co.; 1987.